International Journal of Heat and Mass Transfer 231 (2024) 125807

Contents lists available at ScienceDirect

International Journal of Heat and Mass Transfer

journal homepage: www.elsevier.com/locate/ijhmt

Saturated nucleate pool boiling of cryogenic fluids: Review of databases, assessment of existing models and correlations, and development of new universal correlation

Faraz Ahmad [a], Sunjae Kim [a], Michael Meyer [b], Jason Hartwig [c], Issam Mudawar [a,b,*]

[a] Purdue University Boiling and Two-Phase Flow Laboratory (PU-BTPFL), School of Mechanical Engineering, Purdue University, 585 Purdue Mall, West Lafayette, IN 47907, United States
[b] MTS Inc., 3495 Kent Ave, West Lafayette, IN 47906, United States
[c] NASA Glenn Research Center, Fluids and Cryogenics Branch, Cleveland, OH 44135, United States

ARTICLE INFO

Keywords:
Nucleate pool boiling
Heat transfer coefficient
Cryogens
Models
Correlations

ABSTRACT

The absence of a comprehensive and reliable nucleate pool boiling database for heat transfer coefficient (HTC) of cryogenic fluids is the driving force behind this study. Such a database is essential to evaluating the predictive accuracy of existing tools, including both models and correlations, and to pioneering the development of a new, more accurate predictive method. To address this need, a new Consolidated Cryogenic Nucleate Pool Boiling Database (comprised of 2908 data points) was compiled, with emphasis on HTC from flat horizontal and vertical surfaces, drawing from the broad literature resources available from across the globe. The database enabled a comprehensive assessment of prior models and correlations, and careful examination showed most of these tools yield unacceptably large errors in predicting the HTC data, especially for elevated pressures and large heat fluxes. Consequently, a new correlation is proposed for all cryogenic fluids combined, which is fine-tuned to outperform prior predictive tools, particularly for elevated pressures and large heat fluxes. The new correlation has a Mean Absolute Error (MAE) of 25.36 %, with 64.5 % of the predictions falling within ±30 % of the data and 87.2 % within ±50 %. This exceptional predictive capability positions the new correlation as a robust tool for both thermal design and performance assessment of a broad variety of devices and systems.

1. Introduction

1.1. Applications of cryogenic fluids

Cryogenic fluids play a pivotal role across diverse spheres, encompassing a multitude of applications that permeate our daily lives. Liquid Nitrogen (LN_2), for instance, finds utility in the rapid freezing of food products, as well as in the preservation of tissues and blood for medical purposes. Additionally, it is used in cryosurgery for the targeted elimination of unhealthy tissues. Liquid Oxygen (LO_2) assumes significance in the medical domain, supporting life-sustaining systems. Furthermore, the cooling of superconducting magnets relies heavily on the use of Liquid Hydrogen (LH_2).

In the realm of space exploration and related endeavors, cryogens such as LO_2, LH_2, Liquid Methane (LCH_4), and Liquid Helium (LHe) assume paramount importance. LHe, for instance, plays the critical role of cooling telescopes and satellites orbiting Earth and in maintaining optimal low temperatures required for space-based experiments. Combinations of LO_2 with either LCH_4 or LH_2 find application in ascent stages, descent stages, and in-space fuel depots. LH_2, in particular, serves as an indispensable ingredient in nuclear thermal propulsion systems. Moreover, LH_2 has garnered attention for its potential integration within advanced propulsion systems, acting dually as both propellant and coolant. Fig. 1 in the provided context offers illustrative examples of cryogenic applications in the realm of space exploration [1].

1.2. Fluid physics unique to cryogens

Cryogenic fluids, characterized by markedly low saturation temperatures, form a distinct class of substances that sets them apart from common fluids like water and refrigerants. This differentiation is depicted in Fig. 2 wherein the saturation temperature of various fluids is determined using REFPROP 10 [2]. Moreover, Ganesan et al. [1] have presented a comprehensive comparison of different coolant classes, which reveals notable discrepancies in essential properties of saturated

* Corresponding author.

https://doi.org/10.1016/j.ijheatmasstransfer.2024.125807
Received 4 January 2024; Received in revised form 22 April 2024; Accepted 30 May 2024
Available online 19 June 2024

Nomenclature

C	Constant [dimensionless]; caloric parameter [dimensionless]
c_p	Specific heat at constant pressure [J. kg^{-1}. K^{-1}]
C_{sf}	Empirical constant depending on surface-fluid combination [dimensionless]
D	Diameter [m]
d_b	Bubble diameter [m]
D_b, D_d	Bubble departure diameter [m]
f_d	Bubble departure frequency [s^{-1}]
f_ζ	Foamability constant [dimensionless]
g	Gravitational acceleration [m. s^{-2}]
h	Heat transfer coefficient (HTC) [W. m^{-2}. K^{-1}]
h_{fg}	Latent heat of vaporization [J. kg^{-1}]
h_{nb}	Nucleate boiling heat transfer coefficient [W. m^{-2}. K^{-1}]
h_{nb}*	Dimensionless nucleate boiling heat transfer coefficient (HTC)
h_{nc}	Natural convection heat transfer coefficient [W. m^{-2}. K^{-1}]
K	Vapor-pressure parameter [dimensionless]
k	Thermal conductivity [W. m^{-1}. K^{-1}]
L	Characteristic length [m]
L_b	Bubble length scale [m], $L_b = \left[\frac{\sigma}{g(\rho_f-\rho_g)}\right]^{\frac{1}{2}}$
M	Molecular weight [kg. kmol^{-1}]
N	Nucleation site density [m^{-2}]
N_a	Number of active nucleation sites per unit surface area [m^{-2}]
N_{mol}	Avogadro number $(N_{mol} = 6.022 \times 10^{20})$ [kmol^{-1}]
Nu	Nusselt number; $Nu = \frac{hL}{k_f}$
p	Pressure [N. m^{-2}]
p^*	Reduced pressure; $p^* = \frac{p}{p_{crit}}$
p_{atm}	Atmospheric pressure [N. m^{-2}]
p_{crit}	Critical pressure [N. m^{-2}]
Δp_{sat}	Difference in saturation pressure between wall temperature and saturation temperature, [N. m^{-2}]; $\Delta p_{sat} = p_{sat}\vert_{T=T_w} - p_{sat}\vert_{T=T_{sat}}$
Pr	Prandtl number; $Pr = \mu c_p/k$
q	Heat flow rate [W]
q''	Heat flux from boiling surface [W. m^{-2}]
q''_{nb}	Nucleate boiling heat flux [W. m^{-2}]
R_a	Arithmetic mean of surface roughness profile [m]
$R_{a,p}$	Average roughness parameter of surface profile [m]
Re	Reynolds number
R_{mol}	Molar specific gas constant; R_{mol} = 8314.4598 J. K^{-1}. Kmol^{-1}
R_p	Maximum peak height of surface profile [m]
r_s	Radius of largest cavity on surface [m]
R^*	Surface roughness parameter [dimensionless]
s	Empirical constant accounting for fluid in nucleate boiling correlations [dimensionless]
T	Temperature [K]
T^*	Reduced temperature; $T^* = \frac{T}{T_{crit}}$
T_{crit}	Critical temperature [K]
T_s	Heated surface temperature [K]
T_{sat}	Saturation temperature [K]
ΔT_{sat}	Wall superheat, difference between wall temperature and saturation temperature of liquid [K]; $\Delta T_{sat} = T_w - T_{sat}$
T_w	Heated wall temperature [K]
v	Specific volume [m^3.kg^{-1}]
Z_c	Critical Factor [dimensionless]

Greek symbols

α	Thermal diffusivity [m^2.s^{-1}]; percentage of predictions within ±30 % of the data
β	Percentage of predictions within ±50 % of the data
θ	Contact angle [°]
μ	Dynamic viscosity [kg.m^{-1}.s^{-1}]
ν	Kinematic viscosity [m^2.s^{-1}]
ρ	Density [kg.m^{-3}]
σ	Surface tension [N.m^{-1}]

Subscripts

atm	Atmospheric
b	Bubble
cav	Cavity
crit	Critical
d	Departure
Exp	Experimental (measured)
f	Liquid
g	Vapor
i	Inner
mol	Molar
nb	Nucleate boiling
nc	Natural convection
Pred	Predicted
s	Heating surface
sat	Saturation
w	Heating wall

Acronyms

CFD	Computational fluid dynamics
CHF	Critical heat flux
HTC	Heat transfer coefficient
LAr	Liquid argon
LCH_4	Liquid methane
LH_2	Liquid hydrogen
LN2	Liquid nitrogen
LO_2	Liquid oxygen
MAE	Mean absolute error
MHF	Minimum heat flux
ONB	Onset of nucleate boiling
PU-BTPFL	Purdue University Boiling and Two-Phase Flow Laboratory
RMS	Root mean square

liquid, including liquid density (ρ_f), specific heat at constant pressure ($c_{p,f}$), thermal conductivity (k_f), viscosity (μ_f), Prandtl number (Pr_f), vapor density (ρ_g), latent heat of vaporization (h_{fg}), and surface tension (σ). They highlighted significant variations between cryogens and other fluid classes, though with a few exceptions. They mentioned that cryogens exhibit low ρ_f and ρ_g, high $c_{p,f}$, and low μ_f, σ, and h_{fg}, with LHe displaying the most pronounced deviations. The low saturation temperatures intrinsic to cryogens render them highly susceptible to phase change in most applications, especially those space related. To complete the picture, the critical temperatures and pressures for cryogenic fluids considered in this study are provided in Table 1.

The unique thermophysical characteristics exhibited by cryogens pose considerable challenges when it comes to temperature measurements. This becomes particularly evident in the measurement of quantities like wall superheat ($T_w - T_{sat}$) or wall-to-fluid difference ($T_w - T_f$), where values often approach or fall below 0.5 K. Such measurement

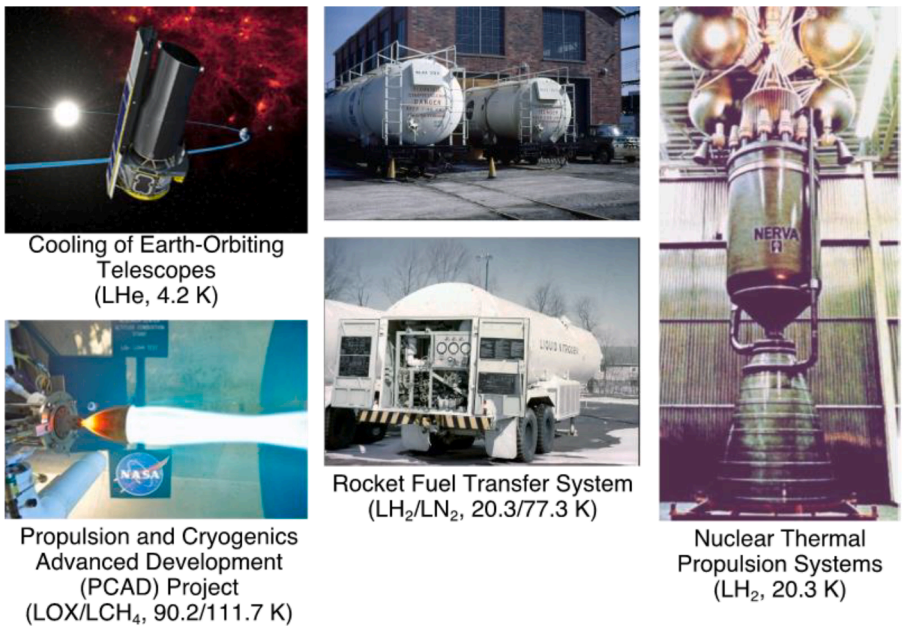

Fig. 1. Examples of applications of cryogens. Adopted from Ganesan et al. [1].

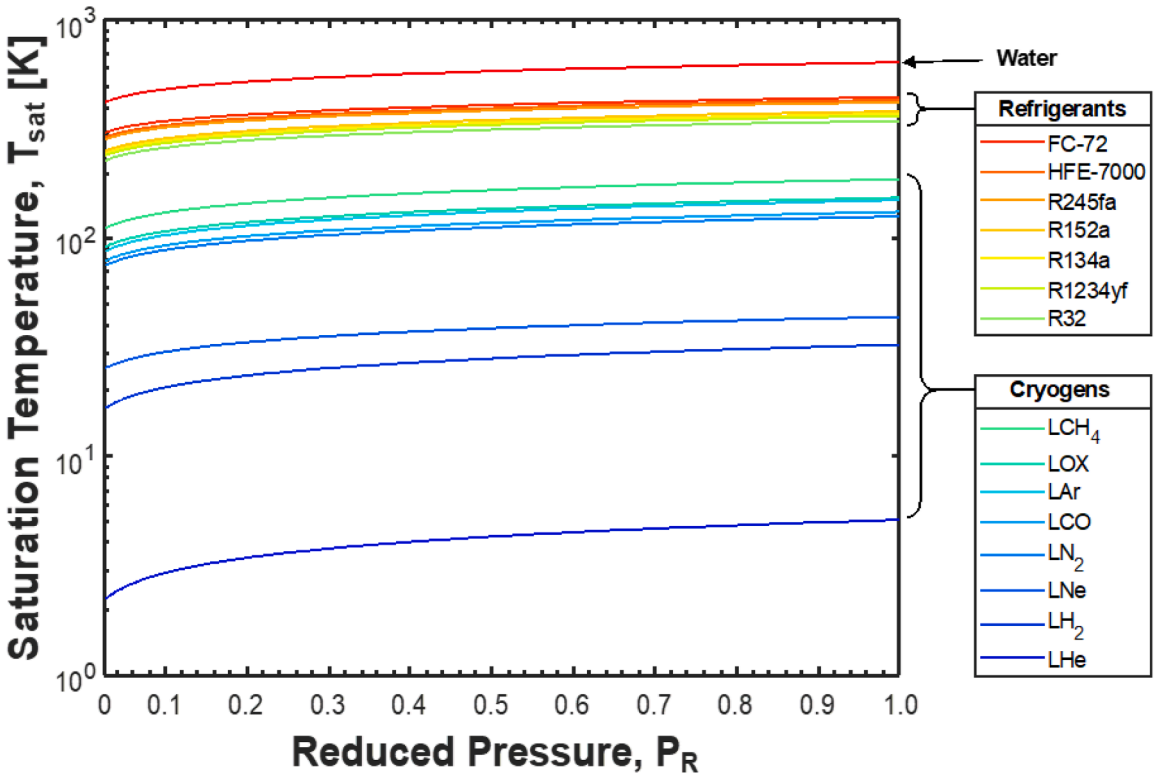

Fig. 2. Classification of coolants into water, refrigerants, and cryogens based on variation of saturation temperature with reduced pressure. Adapted from Ganesan et al. [1].

uncertainties can lead to misleading trends in heat transfer coefficient (HTC) data, resulting in artificial spikes or unphysical values below zero. Two key inferences arise from the challenges associated with temperature measurements: first, researchers must remain cognizant of the likelihood of considerable uncertainties when analyzing cryogenic data and, second, these uncertainties can yield notable difficulties when attempting to construct HTC correlations based on experimental cryogenic data.

1.3. Pool boiling heat transfer

Pool boiling emerges as a remarkably straightforward and economical technique for achieving efficient two-phase cooling. Its versatility allows for widespread implementation across diverse industrial domains, encompassing both low-temperature and high-temperature applications. In low-temperature settings, pool boiling finds extensive use in the cooling of electronic components, power devices, and

Table 1
Critical pressure and temperature of cryogenic fluids.

Cryogen	Critical Temperature [K]	Critical Pressure [MPa]
LHe	5.1953	0.22832
Para-H	32.938	1.2858
LH_2	33.145	1.2964
LN_2	126.192	3.3958
LO_2	154.581	5.043
LCH_4	190.564	4.5992
LAr	150.687	4.863

superconductor coils. This method capitalizes on the remarkable capacity of the coolant's latent heat to effectively dissipate substantial amounts of heat, thereby ensuring that device temperatures remain safely below critical thresholds dictated mostly by material integrity and device reliability. Conversely, in high-temperature applications, pool boiling is commonly employed in the quenching of metal alloy parts during heat treating. The objective here is to attain an optimal microstructure within the alloy, thereby enhancing mechanical properties.

1.4. Background on physics of pool boiling

When a cold fluid comes into contact with a hot solid surface, if the temperature of the solid surface, T_w, exceeds the saturation temperature of the fluid, T_{sat}, boiling can occur. During saturated pool boiling, heat is transferred from the solid surface to the fluid, and this heat transfer can be described by the relation

$$q''_w = h(T_w - T_{sat}) = h\Delta T_{sat} \quad (1)$$

Here, q''_w represents the wall heat flux and h represents the HTC. The magnitude of ΔT_{sat} determines the different heat transfer modes of pool boiling that can take place.

Initially, when the system is in a single-phase liquid state, as both q''_w, and ΔT_{sat} increase, bubbles begin to form on the surface. This transitional stage is known as *incipient boiling* or the *onset of boiling* (ONB). As the wall heat flux continues to increase beyond the ONB point, multiple bubbles form at specific nucleation sites, usually corresponding to wall locations with larger surface cavities. At higher values of q''_w, the amount of vapor produced also increases. Initially, the vapor takes the form of discrete bubbles, but at higher q''_w, it transforms into coalescent vapor columns and jets. The process of nucleate boiling continues until it reaches a threshold called the *critical heat flux* (CHF). At this condition, the coalescence of vapor bubbles on the surface significantly hampers the replenishment of the surface with bulk liquid. This replenishment is crucial for maintaining the balance between the mass of vapor produced and the liquid required to maintain the nucleate boiling processes at the surface. The CHF marks the upper end of the nucleate boiling regime.

1.5. Heat transfer characterization: boiling curve versus quench curve

To understand the different heat transfer mechanisms and stages of pool boiling, researchers often refer to the *boiling curve*. This curve is typically obtained through two different measurement methods: the *steady-state heating method* and the *transient (quenching) method*. The steady-state heating method is widely preferred in pool boiling studies due to its higher accuracy in measuring important heat transfer

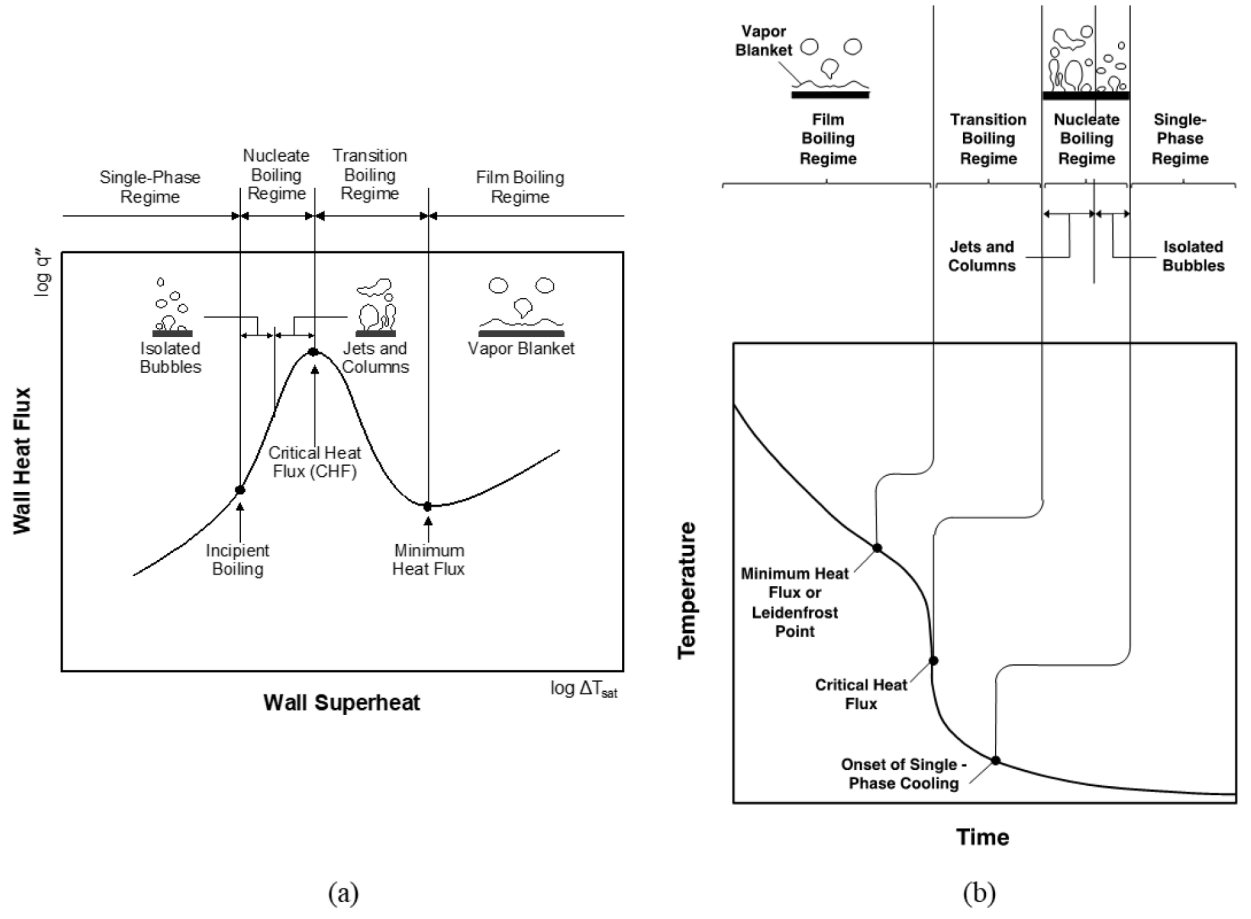

Fig. 3. (a) Pool boiling curve, generally measured using the steady-state heating method. (b) Pool quench curve, generally measured using the transient (quench) method.

parameters.

Using the steady-state heating method, as shown in Fig. 3(a), the boiling curve is generated by conducting tests starting from zero power and gradually increasing or decreasing the wall heat flux in small increments. After each increment, an adequate waiting period is provided to allow the wall temperature to reach a steady state before measurement. This method consists of two steps. In the first step, the wall heat flux is increased incrementally to capture the different regions of the boiling curve, including the *single-phase liquid region*, the ONB point, the *nucleate boiling region*, the CHF point, and the upper portion of the *film boiling region* (following the CHF wall temperature excursion). In the second step, starting from the film boiling condition achieved at the end of the first step, the wall heat flux is gradually decreased to capture the lower portion of the film boiling region, the *minimum heat flux (MHF)* point, which is followed by a sudden decrease in wall temperature towards the nucleate boiling region, followed by the ONB point, and finally, the single-phase liquid region. However, it should be noted that the steady-state method fails to capture the *transition boiling region* of the boiling curve.

The second measurement method involves preheating the wall to a temperature within the film boiling region and then rapidly cooling it in a liquid. This process generates a complete temperature-time (quench) curve, as depicted in Fig. 3(b), which captures all the different boiling regions including transition boiling. It is important to consider that the shape of the quench curve highly depends on the thermal mass of the wall. Eventually, the variation of heat flux with wall superheat for each region is determined by analyzing the transient conduction of the wall, often using a lumped capacitance model.

1.6. Prior postulated nucleate pool boiling mechanisms

Numerous hypotheses have been proposed to elucidate the factors contributing to the remarkable HTCs observed in nucleate boiling. These hypotheses often seek to establish a connection between the heat transfer process and the intricate interfacial behavior that is observed, although they differ greatly in terms of identifying the primary driver for heat transfer. In most models, nucleation is described as originating from small vapor embryos that initially reside within minuscule surface cavities. The growth of these embryos, accompanied by the subsequent release of a bubble from the cavity (referred to as cavity activation), occurs when heat transfer from the surface induces evaporation at the embryo's interface. As a result, the embryo expands within the cavity and eventually beyond its opening. The growing bubble gradually increases in size until its buoyancy overcomes the surface tension force that holds its interface to the surface, causing it to detach. The growth of a bubble initially follows a rapid, inertia-driven phase before transitioning to a slower, thermally controlled phase. It is the intricate mechanisms involved in the initial nucleation of bubbles that are often deemed pivotal to explaining the notably high HTCs achieved during nucleate boiling. Overall, different authors have advocated for vastly distinct dominant mechanisms. Kim [3] comprehensively summarized the diverse heat transfer mechanisms encountered in nucleate pool boiling and made an endeavor to quantify the contribution of each mechanism to heat transfer based on meticulous measurements of local heat transfer at the wall.

Following is a summary of the mechanisms that are commonly accepted as the dominant contributors to heat transfer during nucleate boiling:

i. The mechanism of *near-wall liquid convection* has been widely embraced by numerous researchers when modeling nucleate pool boiling heat transfer [4–6]. This mechanism is based on the premise that the high rate of heat transfer, coupled with the rapid growth and collapse of bubbles, generates significant convective velocities within the liquid region adjacent to the solid wall. Models adopting this mechanism emphasize that most of the heat is directly transferred from the surface to the liquid.
ii. The mechanism of *latent heat transfer* posits that the bubble grows as it absorbs latent heat of vaporization and subsequently releases this heat back to the liquid upon collapse. However, this mechanism is not widely adopted and is only found in a limited number of studies [7,8].
iii. The mechanism of *vapor-liquid exchange* was proposed as an alternative to latent heat transfer by Forster and Grief [7]. According to this mechanism, as the bubble grows, it heats the liquid away from the wall. When the bubble detaches from the wall, it draws an equal volume of cooler bulk liquid towards the surface at a high frequency.
iv. The mechanism of *liquid sublayer evaporation* is based on the hypothesis that the growing bubble entraps a thin liquid micro-layer that wets the surface. Wall heat is predominantly released through heat conduction across this liquid sublayer, contributing to bubble growth through evaporation. The heat is then released through condensation along the top interface of the bubble exposed to the bulk liquid [9]. A fundamental premise of the liquid sublayer evaporation mechanism is that the remarkably high HTCs observed during nucleate boiling are the result of extremely low heat conduction resistance across the thin liquid microlayer.

1.7. Parameters influencing nucleate pool boiling

i. *Surface roughness* is a crucial factor that significantly affects nucleate boiling heat transfer, as recognized by numerous previous researchers. The microtopography of the heating surface, combined with the contact angle, plays a significant role in determining the number of active nucleation sites. Hsu [10] developed a criterion to determine the size of nucleation sites favorable for bubble formation. This criterion compares the superheat available in the liquid thermal layer near the heated wall with the thermodynamic superheat required for bubble growth. Many correlations describe surface microtopography solely in terms of the arithmetic mean of surface roughness, R_a, disregarding other geometric details. However, neglecting these surface details proves inadequate for establishing universal relationships for HTC. For instance, Vachon et al. [11] found that even with the same root mean square (RMS) surface roughness, variations in surface preparation methods lead to noticeable differences in the number of active nucleation sites and the HTCs. When the surface is very smooth (R_a = 0.05–0.4 μm), small changes in surface roughness can result in significant variations in potential nucleation sites and HTC [12]. However, for higher roughness ($R_a \sim 1$ μm), the impact of roughness variations becomes smaller. Interestingly, for surfaces with very large roughness (R_a = 50–100 μm), heat transfer has been reported to increase with increasing roughness as the surface behaves more like one with micro fins rather than a rough flat surface [12]. Another parameter that can affect heat transfer is the presence of a greasy layer on the surface [13]. This effect is most noticeable at CHF and varies depending on the surface orientation.
ii. Another parameter to consider is the *thermal conductivity* of the wall. Due to locally enhanced heat transfer, the surface temperature at active nucleation sites is slightly lower than in non-boiling regions of the surface. Therefore, a material with higher thermal conductivity would reduce the temperature differences between active and non-active regions and allow faster heating of the replenished liquid near the nucleation site. The significance of thermal conductivity depends on the density of nucleation sites – when there are few nucleation sites, the higher local heat flux resulting from higher thermal conductivity has a more pronounced impact on the HTC [12]. Conversely, Bombardieri and

Manfletti [14] compared pool boiling of LN_2 on copper, aluminum, and stainless steel surfaces and observed that the effect of thermal conductivity is less important for rough surfaces with many nucleation sites. It should be noted that highly wetting fluids, such as cryogens, may have fewer nucleation sites on a wall that might be considered rough for less wetting fluids like water [12].

iii. The effect of *subcooling* on nucleate pool boiling heat transfer is a topic of debate among researchers. For instance, Jun et al. [15] investigated the effect of subcooling on water with two different surface materials and reported a trend of increasing CHF with increased subcooling. Lee and Singh [16] noted that the nucleate boiling HTC increased with increasing subcooling at lower wall superheats, but the subcooling effect became negligible at higher superheats. Watwe et al. [17] studied the combined effect of pressure and subcooling on nucleate boiling and reported a very minimal subcooling effect, while increasing pressure decreased the wall superheat. Although the effect on the HTC was minimal, increased subcooling was observed to increase CHF. However, Suroto et al. [18] reported a decrease in the nucleate boiling HTC with increased subcooling. Additionally, Shirai et al. [19] found that increasing the subcooling shifts the boiling curve to the left, i.e., to lower superheat.

iv. The effect of *surface orientation* on nucleate boiling heat transfer performance has been consistently observed by many researchers. For instance, Class et al. [13] investigated pool boiling performance of LH_2 for three different surface orientations (horizontal, vertical, and 45°) and reported that the effect of surface orientation on a smooth surface was almost negligible in the film boiling region. However, as the orientation angle increased from horizontal to vertical, the trend shifted to the left in the nucleate boiling region. Similarly, Zhang et al. [20] observed a decrease in ONB with increasing surface orientation. Howard and Mudawar [21] extensively studied the effect of surface orientation from 0° to 180° on CHF for FC-72 and PF-5052 and found that the effect is not straightforward and cannot be incorporated into a single correlation. They categorized the orientations into three groups: near horizontal facing upward (0° to 60°), near vertical (60° to 165°), and near horizontal facing downward (165° to 180°). They observed that the CHF mechanism differs in each region. In the upward-facing region, vapor motion is greatly influenced by buoyancy, while the near-vertical region exhibits a wavy liquid-vapor interface along the heater surface. However, the downward-facing surface experiences stratification that reduces CHF considerably. Similarly, Priarone [22] conducted experiments with saturated FC-72 and HFE-7100 over a smooth copper surface, varying the surface orientation from 0° to 175°. They confirmed that the HTC increases significantly with increasing orientation angle at lower heat fluxes in the nucleate boiling region. However, the HTC diminishes with increasing angle above 90° for higher heat fluxes. Likewise, Rainey and You [23] immersed a plain surface and a microporous coated surface in FC-72 to investigate the effect of heater orientation on nucleate pool boiling HTC. They found that the effect of heater orientation is significant for a plain surface, but the microporous coated surface was unaffected. They suggested that the insensitivity of the microporous surface is due to the active nucleation sites provided by the porous structure.

v. The effect of fluid *pressure* on nucleate pool boiling heat transfer has received considerable attention from researchers, and a consistent conclusion has been reached: increasing fluid pressure enhances the HTC. Class et al. [13], for instance, reported this observation for nucleate pool boiling of LH_2. However, they also found that the effect of pressure on CHF was non-monotonic, with higher CHF values measured at 0.5 MPa compared to 0.081 and 0.88 MPa. Increasing pressure shifts the boiling curve to the left, resulting in lower superheat at the same heat flux. This trend was confirmed by Akhmedov et al. [24] for LN_2, with pressures ranging from atmospheric to critical pressure. Similarly, Shirai et al. [19] conducted experiments with LH_2, varying the pressure from 0.1 to 1.1 MPa. They compared their results with conventional correlations but found that these correlations overpredicted the effect of pressure on nucleate boiling of LH_2. They reported that increasing pressure increases the HTC until 0.6 MPa. However, beyond 0.6 MPa, the impact of pressure diminishes due to the scarcity of smaller surface cavities capable of accommodating smaller equilibrium diameter bubbles under the high-pressure conditions for LH_2. Expanding on this topic, Bewilogua et al. [25] undertook a comprehensive investigation to explore the influence of pressure on CHF for LH_2, LN_2, and LHe. Their findings revealed a positive correlation between CHF and reduced pressure up to 0.35. Subsequently, the CHF experienced a decline until reaching the critical pressure, and this trend was consistent across all three cryogens. Additionally, Deev et al. [26] conducted a study specifically focused on the effect of pressure on film boiling of LHe. They observed a marginal dependence of pressure on heat flux within the film boiling regime. Comparing their experimental results with a correlation by Kutateladze [27] for CHF, they noted that the deviation remained within 10 % when the reduced pressure was below 0.75. However, a substantial deviation was observed for $P_R > 0.75$.

1.8. Inferences drawn from literature review

Based upon the brief literature review presented above and (detailed discussion of prior models and correlations to follow), several important inferences have emerged. Following are those most obvious:

i. The behavior of the HTC in the nucleate pool boiling regime is remarkably complex and is influenced by numerous variables. Importantly, the influence of certain parameters on the HTC is often non-monotonic and further complicated by influences of other parameters. The complexity here arises from the fact that the impact of any given parameter may be altered significantly when combined with those of other parameters compared to its individual effect alone.

ii. One notably complex influence is that of surface roughness. The impact of this parameter on HTC varies with variations in heat flux level, properties of the fluid, surface material, and surface orientation. In terms of the dependence on heat flux, the effect of surface roughness is more pronounced at lower heat fluxes but far weaker at higher fluxes. And, most importantly, information regarding surface roughness is often either incomplete (e.g., publishing only one measure of the surface roughness while ignoring other potentially important measures) or unavailable. Overall, this renders the task of developing a HTC correlation that is dependent on surface roughness very challenging.

iii. The impact of surface orientation adds another layer of complexity. While most researchers concur that increasing surface inclination from horizontal to vertical enhances the HTC, the degree of sensitivity to this effect is inconsistent among published studies. Additionally, some studies point to the effect of surface orientation being more pronounced for smooth surfaces and less so for rough ones. This underscores the difficulty of developing a HTC correlation that incorporates the effect of surface orientation.

iv. Despite the complex and sometimes conflicting findings regarding the influences of different parameters, the impact of two key parameters, pressure and heat flux, are paramount when developing a new HTC correlation. Two reasons for the necessity to incorporate the effects of these parameters are (a) availability of information on both in virtually all published works, and (b)

Table 2
C_{sf} values for different fluid-surface combinations (not including cryogenic fluids) used in Rohsenow's correlation [35].

Fluid-Surface Combination	C_{sf}
Water–copper	0.03100
Ethyl alcohol–chromium	0.02700
n-Pentane–Emery-polished copper	0.01540
n-Pentane–chromium	0.01500
Water–Emery-polished and paraffin-treated copper	0.01470
Water–chemically-etched stainless steel	0.01330
Water–mechanically-polished stainless Steel	0.01320
Water–platinum	0.01300
Carbon tetrachloride–copper	0.01300
Water–Emery-polished copper	0.01280
n-Pentane–Emery-polished nickel	0.01270
Benzene–chromium	0.01000
Water–ground and polished stainless steel	0.00800
n-Pentane–Emery-rubbed copper	0.00740
Carbon tetrachloride–Emery-polished copper	0.00700
Water–ccored copper	0.00680
Water–brass	0.00600
Water–Teflon-pitted stainless steel	0.00580
35 % K_2CO_3–copper	0.00540
n-Pentane–lapped copper	0.00490
n-Butyl alcohol–copper	0.00305
50 % K_2CO_3–copper	0.00270
Isopropyl alcohol–copper	0.00225

appreciable influence of both on HTC. However, it is worth noting that the influence of these two parameters increases in complexity above high threshold values for both. Therefore, testing a correlation against data for elevated pressures and high heat fluxes is key to validating overall predictive accuracy of the correlation.

1.9. Objectives of the present study

The present investigation is part of efforts to develop predictive tools for the design and performance assessment of cryogenic systems used in propellant generation, storage, transfer, and utilization of the National Aeronautics and Space Administration (NASA). These endeavors encompass a diverse array of applications, scales, and settings, aligning with NASA's forthcoming missions to the Moon and Mars.

More specifically, this study aims to support efforts to formulate detailed heat transfer relations for each region and transition point of the pool boiling curve for cryogens, which are essential to generating a continuous boiling curve (from the single-phase vapor to the single-phase liquid cooling region). As a part of this effort, CHF correlations have already been published by the Purdue University Boiling and Two-Phase Flow Laboratory (PU-BTPFL) team in collaboration with the NASA Glenn Research Center [28]. The current investigation is solely focused on further advancing the technical knowhow to the prediction of heat transfer in the nucleate boiling region for saturated pool boiling from flat horizontal and vertical surfaces.

Overall, the primary objectives of this study can be summarized as follows:

i. Conduct a thorough review of prior models and correlations pertaining to the nucleate pool boiling region.
ii. Compile from reputable worldwide resources a new *Consolidated Cryogenic Nucleate Pool Boiling Database* (referred to hereafter as *Consolidated Database)* encompassing LHe, LH_2, LAr, LN_2, LOX, LCH_4, and parahydrogen.
iii. Assess the accuracy of the prior models and correlations by comparing predictions against the Consolidated Database.
iv. Since most prior models and correlations were developed for non-cryogenic fluids, and therefore are not expected to provide good predictions for cryogens, the present study aims to propose modifications to prior formulations in pursuit of more accurate predictions specifically for cryogens.
v. Investigate the parametric trends of the Consolidated Database to identify gaps in the ranges of key parameters of interest as a basis for recommending future experimental work.
vi. Propose a new correlation capable of accurately predicting the nucleate boiling heat transfer characteristics of different cryogens.

2. Review of prior nucleate pool boiling models and correlations

In the quest to predict the heat transfer coefficient (HTC) for nucleate pool boiling, investigators have embarked upon two distinctive methodologies. The first embraces the utilization of "universal" HTC correlations, which are predicated on a plethora of fluid properties or property groups for multiple fluids and meticulously tailored through the imposition of empirical coefficients and exponents [29–31]. The second, in contrast to the first, not only considers different fluids but also incorporates terms that account for different fluid-surface combinations, including surface roughness [32–34]. By providing a more realistic representation of diverse pool boiling scenarios, the second approach yields a superior degree of predictive accuracy, endowing it with prominence in more recent literature. Unfortunately, as discussed later, studies that provide such information, especially for cryogenic fluids, are quite sparse.

Using the first approach, Kruzhilin [29] pioneered the development of the first correlation for nucleate pool boiling HTC back in 1947. However, over time, this method became less favored due to its failure to account for the influence of different fluid-surface combinations or surface finish.

Employing the second approach, Rohsenow [32] based his HTC model/correlation on the "bubble agitation mechanism." He argued that experimental data clearly indicate that the HTC in nucleate *flow boiling* is independent of flow velocity. Instead, he contended that the HTC must depend on bubble velocity and bubble size, unlike single-phase forced convection, where the HTC is dictated by flow velocity and tube diameter. He further argued that the magnitude of HTC is determined by the bubble agitation mechanism, which involves the departure of a bubble from the heated surface inducing a counterflow of liquid towards the surface, facilitating heat transfer between the surface and the liquid. He postulated that this mechanism is shared by both nucleate flow boiling and nucleate pool boiling. To capture this behavior, he formulated a correlation in terms of the Stanton number, Reynolds number, and liquid Prandtl number wherein the bubble agitation was accounted for through a "bubble Reynolds number" based on bubble diameter and vapor mass velocity. Unlike Kruzhilin, Rohsenow accounted for the effects of fluid-surface combinations (including surface roughness) and contact angle by introducing empirical parameters C_{sf} and s, respectively. He advised users to employ the correlation along with tabulated values for both parameters obtained from experimental data. Table 2 provides representative values of C_{sf} for different fluid-surface combinations, which are adapted from Das et al. [35]. According to Rohsenow, $s = 1.0$ for water versus 1.7 for other fluids. The realistic incorporation of fluid-surface combinations is why Rohsenow's correlation has stood the test of time and remains the most widely used in the heat transfer literature.

McNelly [36] devised a correlation for nucleate pool boiling by employing the assumption of thin liquid layer concentrated resistance adjacent to the heated wall. According to this proposition, the rapid formation of vapor bubbles within the thin layer induces turbulence, which serves as an important driving force behind heat transfer. Leveraging this assumption alongside dimensional analysis, he successfully formulated a correlation for nucleate pool boiling which emphasizes the contribution of bubble agitation, especially the initial growth of the bubble, as the primary governing factor for heat transfer. He accounted for mass transfer from the liquid pool to the heated surface

by incorporating the contribution of latent heat of vaporization, h_{fg}. Additionally, Pr_f was included to capture the heat transfer characteristics of the liquid film adjacent to the wall. Notably, the effects of heater size and orientation were disregarded in his correlation.

Forster and Zuber [37] devised a HTC correlation by leveraging analytical expressions for bubble growth rate and bubble radius in close proximity to the heating surface. A noteworthy revelation from their study is constancy of the product of bubble growth rate and radius. This key finding enabled formulating a Reynolds number for liquid flow along the heating surface and adopting a relation for the HTC similar to that for single-phase flow. They presented Nusselt number (*Nu*) as a function of Reynolds number (*Re*) and Prandtl number, wherein *Nu* and *Re* were defined in terms of bubble characteristic size and radial velocity. While this correlation encompassed fluid properties like other predictive relations, it also incorporated the term Δp_{sat}, the difference between the fluid saturation pressure corresponding to the surface temperature and the fluid saturation pressure corresponding to the liquid pool temperature.

In another study, Nishikawa et al. [38] constructed an analytical model for the boiling process, incorporating various properties of the liquid, including $c_{p,f}$, σ, and k_f. They also incorporated additional factors for a more realistic capture of nucleate boiling behavior. These factors encompassed the influence of buoyancy in the liquid, resulting from the reduction in liquid density near the heating surface, which induces a stirring effect within the liquid. Furthermore, they accounted for the impact of pressure on fluid properties as well as surface condition. The surface condition was captured by inclusion of a "foamability constant" whose magnitude is dependent on the combination of liquid and surface. Notably, they also posited that their HTC relation could be applied to flow boiling with slight modifications.

Lienhard [39] built upon Tien's [40] earlier analytical formulation of the HTC, which considered the upward motion of bubbles causing the rise of liquid from the heating surface. Tien's model yielded a HTC proportional to the square root of nucleation site density (*Na*) and wall superheat (ΔT_{sat}). Lienhard modified Tien's model by constructing a HTC relation proportional to $Na^{1/3}$ and $(\Delta T_{sat})^{5/4}$. He also pointed out that different fluids exhibit varying "pumping capacity," referring to their ability to induce upward liquid flow. To account for such variations, he introduced a correction term that compares the driving head of the specific liquid to that of a reference liquid, typically water.

Mikic and Rohsenow [41] developed a model for nucleate pool boiling based on the mechanism of "transient conduction" in the liquid layer adjacent to the heated surface. They proposed that the departure of bubbles causes bulk liquid at saturation temperature to rush towards the hotter surface, resulting in transient heating of the same liquid. They posited that this process occurs at very high frequency, dictated by the bubble departure frequency, enabling the transient period with very high heat flux to contribute significantly to the heat transfer. Their model exhibited good agreement with experimental data for various fluids, including water, benzene, ethyl alcohol, and n-pentane.

Labunstov [42] developed a semi-analytical HTC model by analyzing the thermal resistance of the thin liquid layer beneath the region of bubble coalescence. His model accounted for the quasi-periodic mixing of bubbles near the heating surface. However, he neglected both the characteristics of the heating surface and the effects of fluid-surface interactions. Despite this limitation, his model provided reasonable predictions within a range of $\pm$ 35 %.

Stephan and Abdelsalam [43] argued that previous HTC correlations considered only a small subset of the numerous factors influencing HTC. To address this weakness, they explored the effects of 12 non-dimensional groups encompassing thermal and physical properties of the working fluid, thermal properties of the heating surface, and construction of the heater. They employed a power law formulation for the HTC and conducted regression analysis on databases for different fluids to determine which dimensionless groups had the most significant impact. They observed distinct variations in nucleate boiling behavior among different fluid types, leading them to conclude that developing separate correlations for each fluid type would yield more accurate predictions than a single universal correlation.

Shiraishi et al. [44] developed correlations for a closed, vertical two-phase closed thermosyphon by focusing on the nucleate boiling in the bottom liquid pool. However, they recognized that boiling within a closed thermosyphon would limit the motion of vapor bubbles, thus affecting the heat transfer. To address this, they related the boiling behavior in the closed thermosyphon to that of an open thermosyphon, where boiling occurs at atmospheric pressure. Experimental results from previous work by Imura et al. [45] on open thermosyphons guided their determination that the HTC in the liquid pool was proportional to the operating pressure raised to the 0.23 power. Their correlation successfully predicted experimental data for water, ethanol, and Freon 113 within a range of $\pm$30 %.

Cooper [46] proposed a simple correlation based on reduced pressure, heat flux, surface roughness, and molecular weight of the fluid. By employing reduced pressure and reduced temperature (determined from the reduced pressure using the Clapeyron equation), he simplified the representation of thermophysical properties. Additionally, he employed the molecular weight (*M*) of the fluid to account for influences of viscosity and thermal conductivity, proposing $\mu_f \propto m^{2/3}$ and $k_f \propto m^{-0.5}$. He also included surface roughness as a logarithmic exponent of reduced pressure, recognizing its heightened significance at low pressures.

Kutateladze is credited with developing nucleate boiling correlations dating back to 1966 [30] and more recently to 1990 [31]. His power-law relations aim to provide predictions for a wide range of fluids, albeit with reduced accuracy, while ignoring surface roughness effects.

Gorenflo et al. [47] conducted pool boiling experiments on horizontal tubes using a variety of hydrocarbons, with a particular focus on surface roughness effects. They proposed a HTC correlation that depends on heat flux, saturation pressure, thermophysical properties of the fluid, and surface roughness. They found that the influence of heat flux on HTC decreased exponentially with increasing pressure. They also observed that the wall material influenced the HTC, with copper surfaces exhibiting better heat transfer than steel surfaces with similar surface finish. However, they did not incorporate wall material properties into their correlation, opting instead to account for surface roughness effects via the maximum height of surface roughness (R_p). Their correlation is applicable within a pressure range of 0.1 bar to 90 % of the critical pressure and $R_p < 10$ μm.

Leiner [48] proposed a generalized correlation to estimate the HTC for nucleate pool boiling of fluids with lesser known properties. He formulated his work using Gorenflo et al.'s [49] experimental data, aiming to estimate the HTC with limited knowledge about the fluid's properties. Leiner achieved this by employing the principles of thermodynamic similarity and introducing "fluid-specific" parameters to fit his correlation to Gorenflo et al.'s data for nearly 50 fluids. Leiner's fluid-specific parameters included critical factor Z_c, caloric parameter *C*, and vapor-pressure parameter *K*. The critical factor (Z_c) depended solely on the critical properties of the fluid, *C* required knowledge of the specific heat of the fluid in liquid form, molar mass, and specific gas constant, while *K* was derived from the slope of the fluid's *p-T* curve. Leiner proposed four versions of the correlation, depending on the availability of fluid parameters. However, his correlation exhibited high deviations from Gorenflo et al.'s [47] data for isopentane, isopropanol, and n-butanol, and was recommended for neither water nor helium. Nonetheless, it produced acceptable results for refrigerants. Overall, the main advantage of Leiner's correlation is its broad applicability. However, although it accounts for surface roughness (R_a), it is applicable only to well-wetted copper surfaces and boiling from horizontal cylindrical heaters.

Pioro [50] employed an approach similar to Rohsenow's [32], considering the effects of surface-fluid combination and contact angle through the parameter C_{sf}. However, Pioro modified the coefficients and exponents, and the correlation was recommended for a variety of fluids

Table 3
Models and Correlations for nucleate pool boiling heat transfer, in chronological order.

Year	Author(s)	Correlation/Model Equation(s)	Notes
1947	Kruzhilin [29]	$h_{nb} = 0.082\left(\frac{k_f}{L_b}\right)\left(\frac{h_{fg}q''_{nb}\rho_f}{gT_{sat}k_f(\rho_f-\rho_g)}\right)^{0.7}\left(\frac{T_{sat}c_{p,f}\sigma\rho_f}{h_{fg}^2\rho_g^2L_b}\right)^{0.33}Pr_f^{-0.45}$ where $L_b = \sqrt{\frac{\sigma}{g(\rho_f-\rho_g)}}$	Ignores effect of fluid-surface combination
1952	Rohsenow [32]	In terms of ΔT_{sat} $h_{nb} = \mu_f h_{fg}\left[\frac{g(\rho_f-\rho_g)}{\sigma}\right]^{1/2}\mathrm{Pr}_f^{-s/r}\left(\frac{c_{p,f}}{C_{sf}h_{fg}}\right)^{1/r}(\Delta T_{sat})^{\frac{1-r}{r}}$ In terms of heat flux, $h_{nb} = \left(\frac{q''_{nb}}{h_{fg}}\right)^{1-r}\left[\frac{\mu_f}{\sqrt{\frac{\sigma}{g(\rho_f-\rho_g)}}}\right]^r\frac{c_{p,f}}{C_{sf}}\mathrm{Pr}_f^{-s}$ where • $r = 1/3$ • $s = n = 1$ for water • $s = n = 1.7$ for other fluids	C_{sf} is an empirical constant that depends on fluid-surface combination and surface roughness
1953	McNelly [36]	$h_{nb} = 0.225\left(\frac{q''_{nb}c_{p,f}}{h_{fg}}\right)^{0.69}\left(\frac{p\ k_f}{\sigma}\right)^{0.31}\left(\frac{\rho_f}{\rho_g}-1\right)^{0.31}$	
1955	Forster & Zuber [37]	$h_{nb} = \frac{0.00122\Delta T_{sat}^{0.234}\Delta p_{sat}^{0.75}c_{p,f}^{0.45}\rho_f^{0.49}k_f^{0.79}}{\sigma^{0.5}h_{fg}^{0.24}\mu_f^{0.29}\rho_f^{0.24}}$	
1960	Nishikawa & Yamagata [107]	$h_{nb} = 8k_f\left(f_\zeta^{\frac{1}{2}}f_p\frac{1}{M^2P}\right)^{\frac{2}{3}}\left(\frac{c_{p,f}\rho_f^2}{k_f\sigma h_{fg}\rho_g}\right)^{\frac{1}{3}}q''^{\frac{2}{3}}_{nb}$ where: $M = 900\frac{1}{m};\ P = 1.699\frac{kcal}{hr}$ f_ζ = foamability constant; $f_\zeta = 1$ for minimally contaminated surfaces $f_p = \frac{p}{p_{atm}}$ is pressure factor	
1962	Tien [40]	$h_{nb} = 61.3k_fPr_f^{0.33}N_a^{0.5}\Delta T_{sat}$	
1963	Lienhard [39]	$h_{nb} = Ck_f\ (Pr_f)^{\frac{1}{3}}\frac{\sqrt{\frac{\sigma g(\rho_f-\rho_g)}{\rho_f^2}}}{\sqrt{\frac{\sigma_{H_2O}g_{H_2O}(\rho_{f,H_2O}-\rho_{g,H_2O})}{\rho_{f,H_2O}^2}}}Na^{\frac{1}{3}}(\Delta T_{sat})^{\frac{5}{4}}$	- C is empirical constant - Compares fluid to reference fluid (water)
1963	Mostinskii [52]	$h_{nb} = 0.1\ p_{crit}^{0.69}q''^{\ 0.7}_{nb}\ F(p^*)$ where $F(p^*) = 1.8\ p^{*0.17} + 4p^{*1.2} + 10p^{*10}$	
1966	Kutateladze & Borishanskiĭ [30]	$h_{nb} = 0.44Pr_f^{0.35}\left(\frac{k_f}{L_b}\right)\left(\frac{\rho_f(p\times10^{-4})}{(\rho_f-\rho_g)\rho_g g h_{fg}\mu_f}q''_{nb}\right)^{0.7}$ where $L_b = \sqrt{\frac{\sigma}{g(\rho_f-\rho_g)}}$	
1969	Mikic & Rohsenow [41]	$h_{nb} = \left[1 - N_aK\left(\frac{\pi D_b^2}{4}\right)\right]h_{nc} + h_b$where • $h_b = 2N_aD_b^2\sqrt{\pi k_fc_{p,f}\rho_f f}$ • $K = \frac{T_{crit}\ln(p^*)}{(1-T_{crit})}$ where N_a is number of active cavies, D_b bubble departure diameter, and f departure frequency • $N_a = r_s^m\left(\frac{h_{fg}\rho_g}{2T\sigma}\right)^m\Delta T_{sat}{}^m$ • $D_b = a\times10^{-4}\left[\frac{\sigma}{g(\rho_f-\rho_g)}\right]^{1/2}\left(\frac{\rho_fc_{p,f}T_{sat}}{\rho_gh_{fg}}\right)^{5/4}$ • $fD_b = 0.6\left[\frac{\sigma g(\rho_f-\rho_g)}{\rho_g^2}\right]^{1/4}$ where • $a = 1.5$ for water • $a = 4.65$ for other fluids	
1970	Danilova [53]	$h_{nb} = C\left(\frac{R_a}{R_{a0}}\right)^{0.2}(0.14 + 2.2p^*)q''^{0.75}_{nb}$where C is empirical constant and R_{a0} is R_a value for standard conditionFor boiling on industrial-quality tubes, they presented simple correlations • For F-12 $h_{nb} = 5.5(0.14 + 2.2p^*)q''^{0.75}_{nb}$ • For F-22 $h_{nb} = 6.2(0.14 + 2.2p^*)q''^{0.75}_{nb}$	
1972	Labunstov [42]	$h_{nb} = 0.075\left[1 + 10\left(\frac{\rho_f}{\rho_f-\rho_g}\right)^{\frac{2}{3}}\right]\left(\frac{k_f^2}{\nu_f\sigma T_{sat}}\right)^{\frac{1}{3}}q''^{\frac{2}{3}}_{nb}$	

(continued on next page)

Table 3 (*continued*)

Year	Author(s)	Correlation/Model Equation(s)	Notes
1979	Imura et al. [45]	$h_{nb} = 0.32\left(\frac{\rho_f^{0.65} k_f^{0.3} c_{p,f}^{0.7} g^{0.2}}{\rho_f^{0.25} h_{fg}^{0.4} \mu_f^{0.1}}\right)\left(\frac{p}{p_{atm}}\right)^{0.3} q''^{0.4}_{nb}$	
1979	Stephan & Preusser [108]	$h_{nb} = 0.01\left(\frac{k_f}{D_d}\right)\left(\frac{q''_{nb} D_d}{k_f T_{sat}}\right)^{0.67}\left(\frac{\rho_g}{\rho_f}\right)^{0.156}\left(\frac{h_{fg} D_d^2}{\alpha_f^2}\right)^{0.371}\left(\frac{\alpha_f^2 \rho_f}{\sigma D_d^2}\right)^{0.35}\left(\frac{\mu_f c_{p,f}}{k_f}\right)^{-0.16}$	
1980	Stephan &; Abdelsalam [43]	$h_{nb} = 0.246\frac{k_f}{D_d}10^{-7} X_1^{0.673} X_3^{1.26} X_4^{-1.58} X_8^{5.22}$ for water	
		$h_{nb} = 0.0546\frac{k_f}{D_d} X_1^{0.67} X_4^{0.248} X_5^{1.17} X_8^{-4.33}$ for hydrocarbons	
		$h_{nb} = 4.82\frac{k_f}{D_d} X_1^{0.624} X_3^{0.374} X_4^{0.329} X_5^{0.257} X_7^{0.117}$ for cryogenic fluids	
		$h_{nb} = 207\frac{k_f}{D_d} X_1^{0.745} X_5^{0.581} X_6^{0.533}$ for refrigerants	
		where:	
		$X_1 = \frac{q''_{nb} D_d}{k_f T_{sat}}$, $X_2 = \frac{\alpha_f{}^2 \rho_f}{\sigma D_d}$, $X_3 = \frac{c_{p,f} T_{sat} D_d^2}{\alpha_f{}^2}$, $X_4 = \frac{h_{fg} D_d^2}{\alpha_f{}^2}$	
		$X_5 = \frac{\rho_g}{\rho_f}$, $X_6 = \frac{c_{p,f}\mu_f}{k_f}$, $X_7 = \frac{\rho_{f,w} c_{p,f,w} k_{f,w}}{\rho_f c_{p,f} k_f}$, $X_8 = \frac{\rho_f - \rho_g}{\alpha_f{}^2}$	
1982	Shiraishi et al. [44]	$h_{nb} = 0.32\frac{\rho_f^{0.65} k_f^{0.3} c_{p,f}^{0.7} g^{0.2}}{\rho_g^{0.25} h_{fg}^{0.4} \mu_f^{0.1}}\left(\frac{p_g}{p_{atm}}\right)^{0.23} q''^{0.4}_{nb}$	
1982	Bier et al. [54]	$h_{nb} = 3.596 \times 10^{-5} p_{crit}^{0.69} (q''_{nb})^{0.7} F(p^*)$	
		where	
		$F(p^*) = 0.7 + 2\,p^*\left(4 + \frac{1}{1-p^*}\right)$	
1982	Nishikawa et al. [38]	$h_{nb} = 31.4\left(\frac{p_{crit}^2}{M * T_{crit}^9}\right)^{\frac{1}{10}} \times F(p^*) \times q_{nb}^{\frac{4}{5}} \times \left(\frac{8R_p}{R_{p0}}\right)^{\frac{(1-p^*)}{5}}$	
		where	
		$F(P^*) = \frac{p^{*0.23}}{(1-0.99p^*)^{0.9}}$, R_{p0} is R_p value for standard condition	
1984	Cooper [46]	$h_{nb} = 55 q''^{0.67} p^{*\left(0.12 - 0.2\log_{10} R_p\right)}\left(-\log_{10} p^*\right)^{-0.55} M^{-0.5}$	
1989	Ueda et al. [55]	$h_{nb} = C_{sf}^{-1} Pr_f^{-1.7}\left(\frac{c_{p,f} q''_{nb}}{h_{fg}}\right)\left(\frac{L_b}{h_{fg}\mu_f} q''_{nb}\right)^{0.7}$	
		where	
		$L_b = \left[\frac{\sigma}{g(\rho_f - \rho_g)}\right]^{\frac{1}{2}}$	
1990	Kutateladze [31]	$h_{nb} = \sqrt[3]{3.37 \times 10^{-9}\frac{k_f}{L_b}\left(\frac{h_{fg}}{c_{p,f} q''_{nb}}\right)^{-2} M_*^{-4}}$	Improved version of Kutateladze & Borishanskiĭ's model
		where	
		$M_* = \left[\frac{\frac{\sigma g}{(\rho_f - \rho_g)}}{\left(\frac{\rho_f}{\rho_g}\right)^2}\right]^{\frac{1}{4}}$	
1990	Gross [56]	$h_{nb} = 55 q''^{0.7}_{nb}\left[\frac{p^{*0.12}}{\left(\left(-\log_{10} p^*\right)^{0.55}\sqrt{M}\right)}\right]$	
1990	Gorenflo et al. [47]	$h_{nb} = h_0 F_q F_p(p^*) F_w$	
		where $F_q = \left(\frac{q''_{nb}}{q''_{nb0}}\right)^n$, $n = 0.9 - 0.3p^{*0.3}$, $q''_{nb0} = 20{,}000\frac{W}{m^2}$	
		$F_p(p^*) = 1.2p^{*0.27} + 2.5p^* + \frac{p}{1-p^*}$ (*valid between* 0.1*bar and* 90%p_c)	
		$F_w = \left(\frac{R_p}{R_{po}}\right)^{2/15}$, $R_{po} = 1\mu m$ (*exponent valid for* $R_p < 10\mu m$)	
1992	Kaminaga et al. [57]	$h_{nb} = 2.2\left(\frac{\rho_g}{\rho_f}\right)^{0.4}\left(R_{a,\,p}^{\frac{(1-p^*)}{5}} h_{nb,\ Kutateladze}\right)$	
		where	
		$h_{nb,\ Kutateladze} = 0.44 Pr_f^{0.35}\left(\frac{k_f}{L_b}\right)\left(\frac{\rho_f\left(p \times 10^{-4}\right)}{(\rho_f - \rho_g)\rho_g g h_{fg}\mu_f} q''_{nb}\right)^{0.7}$,	
		Ra,p is average roughness parameter.	
1993	Leiner et al. [48]	$h^*_{nb} = AF(p^*) q''^{*n}_{nb} R^{*\phi}$	
		where $q''^{\,*}_{nb} = \frac{q''_{nb}}{q''_{nb}00}$, $R^* = \frac{R_a}{L_{00}}$, $p^* = \frac{p}{p_{crit}}$	
		and $q''_{nb}00 = p_{crit}\left(\frac{R}{T_{crit}}\right)^{1/2}$, $L_{00} = \left(\frac{kT_{crit}}{p_{crit}}\right)^{1/3}$	
		$F(p^*) = 43000^{0.15 - 0.3p^{*0.3}}\left(1.2p^{80.27} + \left(2.5 + \frac{1}{1-p^*}\right)p^{*0.3}\right)$	
		where	
		00 *indicated fluid* − *specific scaling units*, $k = R_{mol}/N_{mol}$,	
		$R = R_{mol}/M$	
		$n = 0.9 - 0.3p^{*015}$ for water, $n = 0.9 - 0.3p^{*0.3}$ for other fluids except helium	

(*continued on next page*)

Table 3 (*continued*)

Year	Author(s)	Correlation/Model Equation(s)	Notes
		A can be chosen based on available information for fluid : $A = A_m = 2.351$, *RMS deviation* $\pm$ 40% $A = 1.2063C^{0.2437}$, *RMS deviation* $\pm$ 14.6% $A = 0.6161C^{0.1512}K^{0.4894}$, *RMS deviation* $\pm$ 14.2% $A = 0.4368C^{0.2113}K^{-0.0521}Z_c^{-0.9166}$, *RMS deviation* $\pm$ 13.6% *with* $C = \frac{c_{p,f}M}{R_{mol}}$, $K = -\frac{T^*\ln(p^*)}{1-T^*}$, Z_c = *critical factor*, $T^* = \frac{T}{T_{crit}}$	
1997	Chowdhury et al. [58]	$h_{nb} = 11.43(Re_b)^{0.72}(Pr_f)^{0.42}\left(\frac{\rho_g}{\rho_f}\right)^{0.5}\left(\frac{d_b}{D_i}\right)\left(\frac{k_f}{D_d}\right)$ for water $h_{nb} = 495.7(Re_b)^{0.8}(Pr_f)^{0.5}\left(\frac{\rho_g}{\rho_f}\right)^{0.33}\left(\frac{k_f}{D_d}\right)$ for ethanol $h_{nb} = 6(Re_b)^{0.78}(Pr_f)^{0.48}\left(\frac{\rho_g}{\rho_f}\right)^{0.58}\left(\frac{k_f}{D_d}\right)$ for Freon R-113 where $Re_b = \frac{q''_{nb}D_d}{\rho_g h_{fg}\nu_f}$, D_d is departure diameter and d_b bubble diameter. Note: The 1st correlation was used in this study because it gave best results among the three equations.	
1997	Pioro [50]	$h_{nb} = C^*_{sf}\frac{k_f}{L_b}\left[\frac{q''_{nb}}{h_{fg}\rho_g^{0.5}[\sigma g(\rho_f-\rho_g)]^{0.25}}\right]^{2/3} Pr_f^m$	Uses Rohsenow's model [32] as basis for correlation
1998	El-Genk & Saber [59]	$h_{nb} = (1 + 1.9\varnothing) \times h_{nb,\ Kutateladze}$ where • $h_{nb,\ Kutateladze} = 0.44Pr_f^{0.35}\left(\frac{k_f}{L_b}\right)\left(\frac{\rho_f(p\times10^{-4})}{(\rho_f-\rho_g)\rho_g g h_{fg}\mu_f}q''_{nb}\right)^{0.7}$ • $\varnothing = \left(\frac{\rho_f}{\rho_g}\right)^{0.4}\left[\frac{\rho_g\nu_f}{\sigma}\left(\frac{\rho_f^2}{\sigma g(\rho_f-\rho_g)}\right)^{\frac{1}{4}}\right]^{\frac{1}{4}}$ • $L_b = \left[\frac{\sigma}{g(\rho_f-\rho_g)}\right]^{\frac{1}{2}}$	
2000	Kiatsiriroat et al. [60]	$h_{nb} = C\left(\frac{\mu_f h_{fg}}{L_b\Delta T_{sat}}\right)\left(\frac{c_{p,f}\Delta T_{sat}}{h_{fg}\mathrm{Pr}_f}\right)^n$ where • $L_b = \left[\frac{\sigma}{g(\rho_f-\rho_g)}\right]^{\frac{1}{2}}$ • $\left\{\begin{array}{c} C = 18.688 \text{ for water} \\ C = 17.625 \text{ for ethanol} \\ C = 20.565 \text{ for triethylene glycol (TEG)}\end{array}\right\}$ • $\left\{\begin{array}{c} n = 0.3572 \text{ for water} \\ n = 0.3300 \text{ for ethanol} \\ n = 0.3662 \text{ for triethylene glycol (TEG)}\end{array}\right\}$ Note: The values of ethanol were used in this study because they gave best results	
2003	Ribatski & Jabardo [61]	$h_{nb} = CR_a^{0.2}p^{*0.45}[-\log(p^*)]^{-0.8}M^{-0.5}q''^{\,n}_{nb}$ where C is an empirical constant	

and different surface finishes. In a related paper, Pioro et al. [51] showed their correlation predicted data for ethanol, water, n-heptane, and R-113 with average percent errors of 40 %, 22 %, 13 %, and 47 %, respectively.

Although there exist numerous additional models and correlations beyond those mentioned above, the primary emphasis of this study lies in the evaluation of popular predictive tools rather than delving into the intricacies of origins of all published tools. Consequently, to ensure comprehensive coverage, the said tools, along with others, have been compiled and presented in Table 3, with a concise summary of related information provided in Table 4. Moreover, a compilation of the number of correlations is presented in Fig. 4 based on decade of publication, which shows the maximum number corresponds to the last decade of the 20th century.

Subsequent sections of this study will concentrate on the accumulation of cryogenic data and the subsequent assessment of the aforementioned models and correlations in light of this dataset.

3. New consolidated cryogenic nucleate pool boiling database

3.1. Compilation of saturated nucleate pool boiling data and criteria for exclusion of data points

The current investigation adopts a systematic approach to gather references and data from diverse sources in the published literature, employing a rigorous data mining methodology similar to the one recently employed by Ganesan et al. [62] in compiling cryogen flow boiling CHF data. The primary sources for the present nucleate pool boiling study predominantly include journal articles from reputable publishers (e.g., Springer and Elsevier), NASA Technical Notes, conference papers, and theses spanning the globe.

The amassing of nucleate pool boiling data involves employing two distinct methodologies: (a) by utilizing specialized software such as WebPlotDigitizer [63] to extract numerical values from graphical representations, and (b) by direct extraction from tabular data provided within the published articles. The data available in these sources predominantly consist of boiling curves, where the heat flux is presented in relation to the wall superheat. To determine the HTC, Eq. (1) is

Table 4
Details concerning nucleate pool boiling models and correlations.

Author(s)	Mechanism(s) Considered	Surface Material/ Finish	Fluid(s)	Contact Angle Consideration	Model vs. Correlation	Accuracy
Kruzhilin [29]	Incorporates effect of bubble reference length and superheat required for incipient boiling	Ignores effects of surface-fluid combination	Applicable to multiple fluids	Ignored	Model	−37.4 % to 35.5 %
Rohsenow [32]	Uses analogy with forced convection Based on bubble agitation mechanism Employs bubble Reynolds number based on bubble diameter and vapor mass velocity	Effects of fluid-surface combination accounted for using empirical parameter C_{sf}	Applicable to different fluids, including water, n-heptane, ethanol and R-113	contact angle effect indirectly accounted for empirically	Semi-empirical model	± 20 % depending on surface and fluid properties
McNelly [36]	Initial growth of the bubble is the main controlling factor for HTC Mass transfer from the liquid pool to the heated surface is governed by the latent heat of vaporization	Size, orientation, and surface effects of heater are ignored	Used for variety of liquids including LN_2 at atmospheric pressures, benzene at critical pressure, refrigerants above atmospheric pressure, and water at low pressures	No information of contact angle	Model	Model predictions below 20 % compared to experimental data
Forster & Zuber [37]	*Re* and *Nu* based on bubble radius and radial velocity	Not mentioned	Ethanol, water, n-pentane, and benzene	Not mentioned	Analytical model	
Nishikawa et al. [38]	Based on fundamental physics Accounts for stirring effect of bubble departure, surface condition, and pressure Applicable to forced convection with some modifications	Effects addressed via "foamability constant" which accounts for surface roughness and cleanliness	Applicable to different fluids	Not considered	Model	Not reported
Tien [40]	Correlation was based on laminar stagnation flow mechanism One of the simplest predictive tools	Based mainly on number of nucleation sites No other surface effects considered	Coefficient and exponents mainly derived for water, but claimed to be applicable other fluids with reasonable accuracy	No information on contact angle considered	Semi-empirical model	Not reported
Lienhard [39]	Analytical model depicting upward fluid velocity caused by bubble column	Not material specific	Water, acetone, n-hexane, carbon tetrachloride, and carbon disulfide	Not considered	Analytical model	Not reported
Mostinskii [52]	Uses reduced pressure to represent physical properties	No material effects considered	Reduced pressure used to account for fluid properties	Not considered	Semi-empirical	Not reported
Kutateladze & Borishanskiĭ [30]	Power law relation with empirical coefficient and exponents	Ignores effects of fluid-surface combination	Applicable to different fluids	Not considered	Model	Up to −52.6 % for R-113 on steel surface
Mikic & Rohsenow [41]	Based on transient heat conduction within bulk liquid replacing departing bubble	Incorporates effects of surface finish in terms of active nucleation sites	Water, ethyl alcohol, and n-pentane	Included in correlation for bubble radius	Model	Good predictive accuracy against available experimental results from the literature
Danilova [53]	Assumed no contact between bubbles Heat transfer assumed to take place between heated wall and liquid, and subsequently from liquid to vapor bubble Developed mainly for tube and tube bundles	Uses roughness term for fully developed boiling	Developed only for Freons	Not considered	Semi-empirical	Not reported
Labunstov [42]	Based on mechanisms of micro-layer evaporation and mixing and stirring caused by quasi periodic bubble release	Validated for stainless steel, chrome, nickel, and silver surfaces	Benzene, heptane, ethyl alcohol, and R-22	Not considered	Analytical model with coefficients fitted to data	Mean error of 25.3 % for water on aluminum surface
Stephan & Abdelsalam [43]	Dimensionless power law correlation of fluid and heating surface parameters	Validated for copper, brass, platinum, nickel, stainless steel, chromium, and various plating methods	Water, benzene, ethanol, n-pentane, n-heptane, n-hexane, n-butanol, diphenyl meta-terphenyl, ortho-terphenyl, helium, hydrogen, nitrogen, oxygen, neon, methane, argon, R-12,	Assumes $\theta = 45^{\circ}$ for water, 35° for refrigerants and hydrocarbons, and 1° for cryogenic fluids	Correlation	Predicted *Nu* off by 11.3 % for water, 12.2 % for hydrocarbons, 14.3 % for cryogenic fluids, and 10.57 % for refrigerants

(*continued on next page*)

Table 4 (*continued*)

Author(s)	Mechanism(s) Considered	Surface Material/ Finish	Fluid(s)	Contact Angle Consideration	Model vs. Correlation	Accuracy
			R-114, R-113, RC318, R-11, propane, and carbon dioxide			
Shiraishi et al. [44]	Applicable to thermosyphons	Performed in copper tube	Water, ethanol, and R-113	not considered	Correlation	Within 30 %
Cooper [46]	Simplified formulation in terms of few dimensionless groups	Accounts for surface finish in relation to reduced pressure	Not provided	Not considered	Correlation	
Ueda et al. [55]	Applicable to thermosyphons	Fluid-surface combination accounted for using empirical parameter C_{sf}	Water, methanol, R113	Not considered	Correlation	Good agreement with the authors' own experimental data
Kutateladze [31]	Limited in applicability	Not considered	Tested against data for different fluids	Not considered	Model	124.1 % error for water on aluminum surface
Gross [56]	Uses 2529 data points from previously published literature to develop a correlation for thermosyphon	Surface roughness unknown yet authors assumed a constant value of R_a =1 μm	Based on data for 11 different fluids including refrigerants, water, and alcohol	0° to 85°	Correlation	63 % of data within 30 %. 89 % of data within 50 %
Gorenflo et al. [47]	Function of saturation pressure, heat flux, and to a lesser extent wall material and roughness	Validated for copper, brass, mild steel, and stainless-steel surfaces with Emery ground, sandblast, and drawn surface treatments	Hydrocarbons with saturation pressures between 0.3 and 39 bar	Not considered	Correlation	
Leiner et al. [48]	Employs thermodynamic similarity using fluid-specific parameters	Validated for copper Accounts for surface roughness	Correlation suggested for fluids with lesser-known properties Good accuracy for R-21, R-113, and R-114 Deviations from data for isopentane, isopropanol, and n-butanol Less accurate for water, ammonia, and helium	Not considered Study concerns only well-wetted copper surface	Correlation with mathematical modeling	±40% for no fluid-specific parameter model ±14.6% for one parameter (C) model ±14.2% for two parameter (C, K) model ±13.8% for three parameter model (C, K, Z_c)
Chowdhury et al. [58]	Developed for vertical small diameter tube with water as working fluid	Not considered	Water, ethanol, R-113	Not considered	Correlation	Compared to prior correlations, HTC was found to be larger than for pool boiling correlations and smaller than for heat pipe correlations
Pioro [50]	Modified form of Rohsenow's original model [32]	Effects of fluid-surface combination accounted for using empirical parameter C_{sf}	Applicable to different fluids	Contact angle effect indirectly accounted for empirically	Semi-empirical model	−5 % to 6.5 % for different fluid-surface-combinations
El-Genk et al. [59]	Modified form of Kutateladze correlation by introducing a mixing coefficient The mixing coefficient accounts for mixing between bubble generated in the pool and bubble rising along the wall	Not considered	Methanol, ethanol, water, R-113, R-11, and Dowtherm-A	Not considered	Correlation	within 15 % of experimental data
Kiatsiriroat et al. [60]	Developed for thermosyphons	Not considered	Water, ethanol, and triethylene glycol (TEG).	Not considered	Correlation	Not reported

employed. Alternatively, in certain papers, the HTC information is directly provided in relation to the heat flux; here, the wall superheat is calculated also using Eq. (1). To ensure accuracy and reliability, the lowest and highest data points within the nucleate boiling region, representing ONB and CHF, respectively, are deliberately excluded from analysis. This cautious approach aims to focus solely on the region of nucleate boiling and exclude the regions of natural convection, transition boiling, and film boiling.

The process of acquiring references for the data mining endeavor encountered several challenges, including (a) unavailability of certain references when utilizing Purdue University's Interlibrary Loan (ILL) services, (b) hesitation of certain investigators to share their own data, and (c) the occurrence of duplicate data. To ensure data mining integrity, a meticulous examination of data from the various sources was conducted to identify and eliminate any duplicates. Moreover, given the primary focus of this study on saturated nucleate pool boiling from flat surfaces, data for pool boiling on wires, tubes, or cylinders, or along narrow channels are intentionally excluded from consideration. Following the initial phase of excluding duplicate data, attention was then directed towards excluding additional data that do not meet the following criteria:

1. Only data for pure cryogenic fluids are considered; data for fluid mixtures and non-cryogenic fluids are excluded.

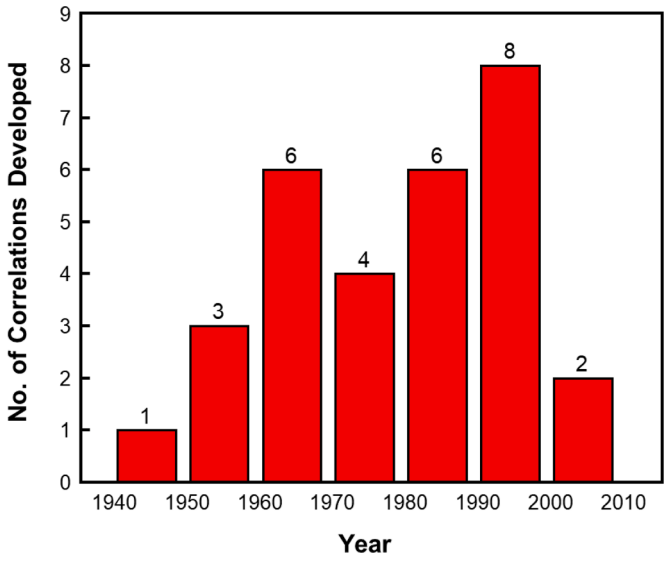

Fig. 4. Decade-based distribution of correlation development.

2. Only saturated nucleate pool boiling data are considered; data for other pool boiling regions are excluded.
3. Only pool boiling on uniformly heated flat surfaces, including those both 'infinite' and finite.
4. Only steady-state pool boiling data are included, while quench data are excluded due to limited availability, complexity, and compromised reliability stemming from the large and rapid variations in wall temperature in quenching experiments.
5. Only data for subcritical pressures and temperatures and saturation conditions are considered.
6. Only data from horizontal and vertical surface orientations are considered for analysis.
7. Only data measured in Earth gravity are considered. Data for microgravity or hyper-gravity are excluded until such data are available from parabolic flight experiments to eventually address the effect of gravity on HTC.
8. Data from both smooth and roughened heating surfaces are considered; data from finned or coated surfaces are excluded.
9. Only datapoints for which all information necessary for correlating the data is provided, such as operating pressure, heat flux, wall temperature, and surface orientation angle.

Application of these criteria resulted in the refinement of the database to include only datapoints that are relevant and suitable for analysis. A comprehensive overview of the data acquired and those excluded from consideration is provided in Table 5.

3.2. Final consolidated cryogenic nucleate pool boiling database

The primary objective of this endeavor is to provide the reader with comprehensive information about cryogenic nucleate pool boiling. Although this study focuses on this specific boiling regime, data for other regimes were also amassed to cover the entire boiling curve, which will be the subject of forthcoming research articles from the Purdue University Boiling and Two-Phase Flow Laboratory (PU-BTPFL). *The data considered in this study are specific to cryogenic saturated pool boiling from flat horizontal and vertical surfaces.*

In the initial data mining, 9665 datapoints were amassed from 48 references. The collected data were then segregated based on boiling regime, cryogen, subcooling, surface orientation, and gravitational acceleration as depicted in Fig. 5(a). Following this initial phase, the exclusion criteria outlined in Table 5 were applied to further refine the database, resulting in creation of the *Consolidated Cryogenic Nucleate Pool Boiling Database* (*Consolidated Database* for short). A summary of the final Consolidated Database is presented in Fig. 5(b).

The final Consolidated Database comprises a total of 2908 nucleate pool boiling data points sourced from 48 references, encompassing seven cryogens: LHe, LN_2, LH_2, LOX, LAr, LCH_4, and parahydrogen as detailed in Table 6. The fluid distribution of data points is as follows: LN_2 (1417), LHe (650), LOX (307), LH_2 (246), LAr (142), para-H (77), and LCH_4 (69). Furthermore, 85.8 % of the datapoints correspond to the horizontal upward facing surface orientation ($\theta = 0°$), while the remaining 14.2 % pertain to the vertical orientation ($\theta = 90°$). Excluded from the final Consolidated Database are 402 subcooled datapoints, 11 microgravity datapoints, and 92 hyper-*g* datapoints, which will be the focus of upcoming studies by the authors.

4. Assessment of existing models and correlations

After conducting a meticulous literature review, a total of 30 different models and correlations have been compiled, as shown in Table 3. To facilitate the assessment process, these correlations have been categorized into three distinct groups.

The first group, designated as Category 1, comprises correlations for which data for all parameters included in the correlations are readily available. The evaluation of these correlations is deemed the most comprehensive and reliable. The second group, Category 2, consists of correlations wherein certain parameters are missing from some databases, such as surface roughness. Lastly, Category 3 comprises correlations that involve specific parameters such as nucleation site density (*Na*), wall properties, etc., for which no data is currently available in the Consolidated Database. The Category 3 correlations are presented for the sake of completeness but not evaluated due to the absence of essential information.

4.1. Statistical parameters and methodology for assessment

The Consolidated Database is used to evaluate the accuracy of all the reviewed models and correlations in predicting the nucleate boiling heat transfer coefficient (HTC). In this assessment, three different statistical parameters are employed: mean absolute error (MAE), percentage of datapoints predicted within ±30 % of experiment, α, and percentage of datapoints predicted within ±50 % of experiment, β. REFPROP 10 [2] is used to obtain thermophysical properties of the relevant fluids at different pressures and temperatures. MAE, in this context, is defined as the average absolute difference between the predicted value from the model or correlation and the corresponding experimental value in the Consolidated Database divided by the experimental value,

$$MAE = \frac{1}{N}\sum \frac{\left|HTC_{Pred} - HTC_{Exp}\right|}{HTC_{Exp}} \times 100\% \quad (2)$$

By employing these different statistical parameters, the assessment process aims to provide a robust analysis of the predictive capability of the reviewed models and correlations.

4.2. Detailed assessment of Rohsenow's correlation and suggested c_{sf} values for cryogens

The Rohsenow correlation [32], a venerable and foundational correlation, holds great significance in forecasting nucleate pool boiling performance, evidenced by its unmatched popularity in both research articles and textbooks. It is for these reasons that this correlation is given special attention in the present study.

As indicated earlier, the Rohsenow's correlation involves the term C_{sf} which relies on diverse surface-fluid combinations. Das et al. [35] compiled a list of recommended C_{sf} values, as presented in Table 2, albeit for only non-cryogenic fluids because of severe shortage of cryogenic data. Clearly, there exists a dearth of suggestions regarding C_{sf}

Table 5
Summary of total cryogenic nucleate boiling datapoints acquired from individual sources and those excluded from consideration, along with reasons for the exclusion.

Article no.	Year	Reference	Total Acquired Datapoints	No. of Excluded Datapoints	Reasons for Excluded Data
1	1960	Class et al. [13]	92	47	• Greased surface (13 points) • Film boiling data (34 points)
2	1963	Kosky et al. [64]	72	72	• CHF data (72 points)
3	1964	Lyon et al. [65]	145	8	• Critical pressure data (8 points)
4	1965	Graham et al. [66]	211	134	• Unidentifiable data (31 points) • Supercritical pressure data (64 points) • CHF data (2 points) • Hyper-g data (37 points)
5	1965	Lyon et al. [67]	81	81	• CHF data (81 points)
6	1965	Lyon et al. [68]	198	198	• Pressure not defined (198 points)
7	1966	Cummings et al. [69]	17	17	• CHF data (17 points)
8	1966	Kosky [70]	2233	1443	• CHF data (154 points) • Mixture data (485 points) • R-12 data (160 points) • Supercritical pressure data (177 points) • Transient effects (420 points) • Data involving use of fiber glass insulation between test element and heater (47 points)
9	1967	Clark et al. [71]	45	45	• Film boiling data (45 points)
10	1968	Marto et al. [4]	97	16	• Grease coating data (8 points) • Teflon coating data (8 points)
11	1969	Butler et al. [72]	3	3	• CHF data (3 points)
12	1970	Merte [73]	345	204	• CHF data (15 points) • Data with pressure variations (10 points) • Natural convection data (36 points) • Transition boiling data (73 points) • Film boiling data (70 points)
13	1970	Porchey et al. [9]	72	72	• CHF data (72 points)
14	1971	Jergel et al. [74]	78	32	• Channel data (32 points)
15	1974	Akhmedov et al. [24]	171	64	• Data above 2.5 MPa were not considered because authors mention the accuracy of measuring heat flux was very low at high pressures (64 points)
16	1974	Grigoriev et al. [75]	143	0	• No data excluded
17	1974	Jergel et al. [76]	53	0	• No data excluded
18	1974	Swanson et al. [77]	23	11	• Natural convection data (3 points) • Film boiling data (8 points)
19	1975	Bewilogua et al. [25]	164	155	• CHF data (109 points) • Orientation other than horizontal or vertical (46 points)
20	1975	Warner et al. [78]	62	0	• No data excluded
21	1976	Grigoriev et al. [79]	207	207	• Boiling in tubes
22	1976	Vishnev et al. [80]	27	5	• Coating data (9 points)
23	1977	Deev et al. [26]	166	64	• Film boiling data (57 points)
24	1977	Ishigai et al. [81]	198	99	• Natural convection data (99 points)
25	1977	Ogata et al. [82]	53	48	• Film boiling data (14 points) • Natural convection data (14 points) • Hyper-g data (20 points)
26	1978	Ibrahim et al. [83]	270	237	• Film boiling data (8 points) • Subcooled data (229 points)
27	1980	Verkin et al. [84]	226	226	• CHF data (32 points) • Natural convection data (42 points) • Pool temperature not provided (152 points)
28	1981	Ogata et al. [85]	59	35	• Film boiling data (35 points)
29	1986	Nishio et al. [86]	425	415	• Film boiling data (318 points) • Transition boiling data (86 points) • Transient data (11 points)
30	1988	Beduz et al. [87]	134	88	• Grooved and drilled surface (52 points) • Plasma sprayed surface (36 points)
31	1989	Chandratilleke et al. [88]	252	252	• Teflon coating data (137 points) • SS304 coating (50 points) • Film boiling data (65 points)
32	1989	Nishio & Chandratilleke [89]	121	29	• Orientation other than horizontal or vertical (4 points) • Film boiling data (25 points)
33	1990	Ashworth et al. [90]	614	565	• R-12 data (166 points) • Porous coating data (399 points)
34	1991	Kirichenko et al. [91]	58	58	• CHF data (58 points)
35	1992	Kozlov & Nozdrin [92]	89	54	• Film boiling data (49 points) • CHF data (5 points)
36	1993	Ogata & Mori [93]	243	243	• Coating data (121 points) • Film boiling data (46 points) • Transition data (76 points)
37	1998	Iwamoto et al. [94]	259	131	• Film boiling data (131 points)
38	2000	Nguyen et al. [95]	80	5	• Orientation other than horizontal or vertical (5 points)
39	2002	Hata et al. [96]	150	150	• CHF data (150 points)

(*continued on next page*)

Table 5 (*continued*)

Article no.	Year	Reference	Total Acquired Datapoints	No. of Excluded Datapoints	Reasons for Excluded Data
40	2002	Ohira & Furomoto [97]	108	96	• Triple point pressure data (35 points) • Slush data (35 points) • Natural convection data (26 points)
41	2004	Duluc et al. [98]	40	40	• Natural convection data (10 points) • Data for pentane, quench data (30 points)
42	2009	Jin et al. [99]	180	180	• Natural convection data (15 points) • Transition boiling data (39 points) • Film boiling data (97 points) • NB data (29 points)
43	2009	Wang et al. [100]	103	0	• No data excluded
44	2010	Shirai et al. [19]	433	277	• Natural convection data (87 points) • Un-developed nucleate boiling (150 points) • CHF data (40 points)
45	2011	Jin et al. [101]	159	127	• Inconsistent data (127)
46	2015	Balakin et al. [102]	193	72	• Natural convection data (45 points) • Film boiling data (27 points)
47	2016	Bombardieri et al. [14]	44	0	• No data excluded
48	2016	Zoubira et al. [103]	21	0	• No data excluded

values for cryogenic fluids. Only a few studies have provided guidance concerning use of Rohsenow's correlation for cryogens. For example, Barron and Nellis [105] proposed a value of 0.013 for all cryogens except LHe, while Holdredge and McFadden [106] conducted a study specifically for LHe and recommended a C_{sf} value of 0.169 for LHe-I. The elevated C_{sf} value for LHe may be attributed to the afore-mentioned appreciable departure of LHe properties from those of the other cryogens. Consequently, this section of the paper will provide a thorough examination of the selection process for C_{sf} values for cryogenic fluids, with special attention given to LHe.

To begin the analysis, initial values of 0.169 for LHe and 0.013 for all other cryogens were employed to evaluate the Rohsenow's correlation against the present Consolidated Database, by first conducting the assessment for horizontal and vertical surface orientations separately. Using these C_{sf} values, the correlation yields a MAE of 39.06 % for horizontal orientation, Fig. 6(a), 43.48 % for vertical orientation, Fig. 6 (b), and 39.68 % for both orientations combined, Fig. 6(c), which shows a rather weak dependence on surface orientation. However, it is evident that the correlation consistently underpredicts the LHe data, indicating the need to further revise the C_{sf} value specifically for LHe.

Employing a trial-and-error approach, various C_{sf} values ranging from 0.013 to 0.169 were tested for LHe. Fig. 7 shows how, when combining data for both horizontal and vertical orientations, the least MAE of 29.23 % is achieved when using $C_{sf} = 0.048$ for LHe while maintaining the same previous value of $C_{sf} = 0.013$ for all other cryogens. These values of C_{sf} show best overall predictions when using Rohsenow's correlation.

In an attempt to further simplify and establish universality in the application of Rohsenow's correlation, a single C_{sf} value is attempted for all cryogens, including LHe, and both orientations combined. To achieve this goal, the common value of C_{sf} was varied within the range of 0.12 to 0.05, and the corresponding MAE was calculated for each value. The corresponding least MAE of 56.86 % is achieved when using $C_{sf} = 0.023$. The greatly increased MAE compared to that in Fig. 6(c) shows conclusively that C_{sf} value for LHe should not be consolidated with that for the other cryogens.

Another approach to assessing the utility of Rohsenow's correlation is attempted wherein different values of C_{sf} were optimized for each cryogen separately. To test this hypothesis, C_{sf} values were varied individually in the range of 0.011 to 0.05. Notably, as detailed in Table 7, it is observed that optimum C_{sf} values for the vertical orientation are a bit lower than those for the horizontal orientation, but the differences are small. Overall, the results in Table 7 confirm that (i) the optimum value of C_{sf} for LHe is significantly different from those for the other cryogens, and (ii) optimum values for the other cryogens are comparatively close to one another.

4.3. Assessment of category 1 models and correlations

As previously discussed, the prior models and correlations have been divided into three distinct categories. Category 1 models and correlations are assessed against the entire Consolidated Database of 2908 datapoints because they include parameters that are fully represented in the Database. Most of the parameters are thermophysical properties that are conveniently derived from the operating conditions, mainly operating pressure. This category comprises 19 correlations, so presenting them all in a single figure proved challenging. Consequently, Category 1 is further subdivided into sub-groups based solely on range of MAE. It is important to note that this sub-categorization is intended primarily for convenience of the reader in comprehending the presented plots.

Fig. 8 shows Category 1 models and correlations yielding a MAE lower than 45 % for horizontal and vertical orientations combined; these represent the most accurate in the published literature. Notably, Rohsenow's correlation, Fig. 7, using the aforementioned values of $C_{sf} = 0.48$ for LHe and 0.013 for all other cryogens, is shown performing exceptionally well, with a MAE of 29.23 %. It is worth highlighting that this is the only correlation in the existing literature yielding a MAE below 30 %. Following Rohsenow's, the models/correlations by Kruzhilin [29], McNelly [36], Kutateladze [31], Chowdhury et al. [58], and Kutateladze and Borishanskiĭ [30] also performed reasonably well, with MAEs of 30.51 %, 31.03 %, 33.53 %, 34.59 %, and 42.07 %, respectively.

Fig. 9 shows predictions for Category 1 models and correlations yielding a MAE higher than 45 % for horizontal and vertical orientations combined. It shows moderately accurate predictions by Imura et al. [45], Pioro [50], Nishikawa and Yamagata [107], Danilova [53], El-Genk et al. [59], and Stephan and Abdelsalam [43], with MAEs of 45.32 %, 47.89 %, 51.63 %, 51.95 %, 53.15 %, and 58.50 %, respectively. It must be noted that because Pioro's correlation lacks recommendations for C_{sf} and the liquid Prandtl number exponent, m, values of both were determined in the present study through trial and error in pursuit of lowest MAE. However, Fig. 9 shows both this correlation and Nishikawa and Yamagata's greatly underestimate HTCs for both LH_2 and LHe. Additionally, it is important to note that Danilova's original correlation belongs to Category 2 due to its inclusion of a surface roughness term which is lacking for most datapoints in the Consolidated Database. However, Danilova also proposed a correlation specifically for Freon 22 that excludes the surface roughness term; it is this modified correlation that is included in Category 1 and whose predictions are provided in Fig. 9.

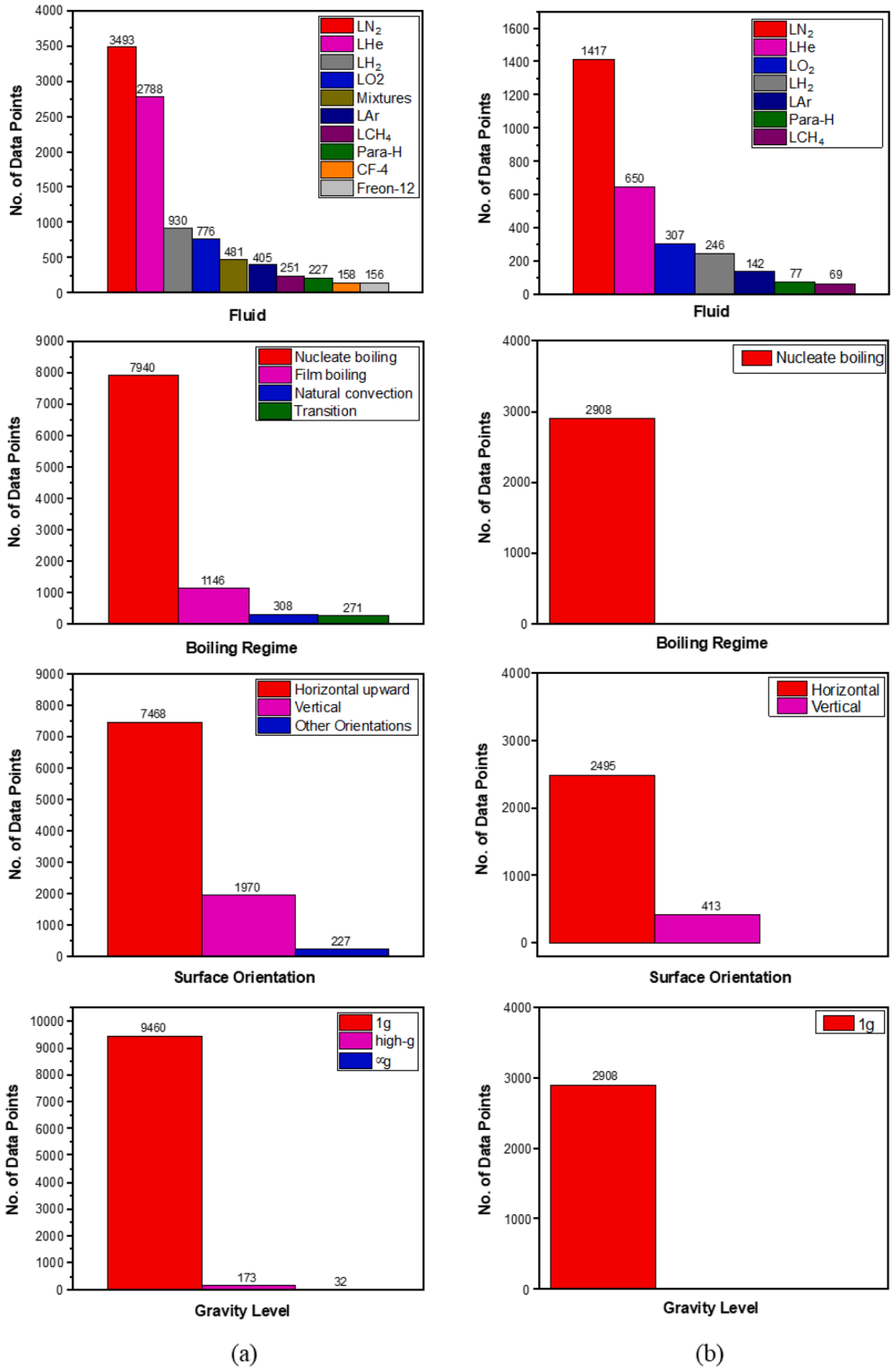

Fig. 5. Summary of Consolidated Database (a) before applying exclusion criteria and (b) after applying exclusion criteria.

Table 6
Summary of Consolidated Cryogenic Nucleate Pool Boiling Database.

Reference	Acceptable Nucleate Boiling Datapoints	Heater Geometry	Heater Size: Width x Length [mm^2] or Diameter (Thickness) [mm]	Heater Material	Surface roughness [μm]	Pressure [MPa]	Inclination Angle	Boiling State
Liquid Nitrogen								
Lyon et al. [65]	56	Flat ring	ID – 64.5 OD – 68.5 (0.0508)	Platinum	Not mentioned	0.0419 – 2.5382	0°	Saturated
Kosky [70]	387	Circular	19.05	Platinum	Polished	0.1019 - 3.3532	0°	Saturated
Marto et al. [4]	81	Circular	25.4 (21.08, 9.093)	ETP copper; nickel	Mirror finish; roughened;	0.1013	0°	Saturated
Merte [73]	131	Circular	76.2 (20.64)	Copper	Polished 600 grit	0.0986	0°; 90°	Saturated
Akhmedov et al. [24]	107	Circular	10	Cr18Ni9Ti steel, M-1 copper	Not mentioned	0.1 – 3.2	0°	Saturated
Swanson & Bowman [77]	12	Circular	12.7	Sapphire	Not mentioned	0.1013	0°	Saturated
Bewilogua et al. [25]	3	Circular	24.98	Copper	0.2 (ground with F9 Emery cloth)	0.0983 – 1.965	0°	Saturated
Warner & Park Jr. [78]	62	Circular	38.1 (3.81)	Gold plated copper	Not mentioned	0.0993	0°	Saturated
Ishigai et al. [81]	99	I -shaped	10 (0.1)	Stainless steel	2, 3, rolled	0.1013	0°	Saturated
Nishio [86]	10	Circular	22 (60)	Oxygen free copper	Not mentioned	0.1013	0°	Saturated
Beduz et al. [87]	46	Square	50 × 50 (6)	Aluminum, copper	Mirror polished	0.1013	0°	Saturated
Ashworth et al. [a] (1990) [90]	15	Square	25.4 × 25.4 (5)	Aluminum	Smooth	0.1013	90°	Saturated
Nguyen et al. [95]	75	Rectangular	20 × 10 (2.54)	Copper	Confinement spacing of 2.5mm	0.1013	0°; 90°	Saturated
Ohira & Furumoto [97]	12	Circular	25	ETP copper	Less than 1	0.0125, 0.1013	0°	Saturated
Wang et al. [100]	103	Circular	32	Copper	Not mentioned	0.1013	0°	Saturated
Jin et al. [101]	32	Circular	9, 12, 15	Copper (99.9 %), brass (Cu 60.5–63.5 %, rest Zn), Aluminum alloy (Si 0.2–0.6 %, Fe 0.35 %, Mg 0.45–0.9 %, rest Al)	Polished	0.1013	0°	Saturated
Balakin et al. [102]	121	Rectangular	(25–40) x 2.5, (0.08)	Ni – W tape	Not mentioned	0.1013	0°; 90°	Saturated
Bombardieri & Manfletti [14]	44	Rectangular	46 × 51	Copper, Aluminum, Stainless steel	0.076, 0.141, 0.117	0.09815	0°	Saturated
Zoubira et al. [103]	21	Rectangular ribbon	100 × 4 (0.025)	Brass	Not mentioned	0.1013	0°	Saturated
	1417	***Total acceptable datapoints for*** LN_2						
Liquid Helium								
Jergel & Stevenson [74]	46	Circular	15 (10)	OFHC Copper	Not mentioned	0.1013	0°; 90°	Saturated
Grigoriev et al. [75]	143	Circular	8	Copper M-1, bronze 6.5–0.15, nickel H-1, brass πM-62, stainless steel X18H9T	1–10	0.1	0°	Saturated
Jergel & Stevenson [76]	53	Circular	15 (10)	Al 69 [99.9999 %]	Not mentioned	0.1013	0°; 90°	Saturated
Bewilogua et al. [25]	6	Circular	24.98	Copper	0.2	0.0064 – 0.2178	0°: 90°	Saturated
Vishnev et al. [80]	18	Rectangular	96 × 10.4 (0.063)	Stainless steel	Not mentioned	0.1013	0°; 90°	Saturated
Deev et al. [26]	102	Square	30 × 30	Copper (99.993 %)	0.08 (polished) 0.3 (rough)	0.1 – 0.2258	0°, 90°	Saturated
Ogata & Nakayama [82]	5	Circular	6.1	Copper	Polished	0.101	0°	Saturated
Ibrahim et al. [83]	33	Circular	25.4 (31.75)	OFHC Copper	Not mentioned	0.0983 – 0.1307	0°	Saturated, subcooled
Ogata & Nakayama [85]	24	Square	15 × 15	Copper	Smooth; oxidized smooth	0.1013	0°	Saturated
Nishio & Chandratilleke [89]	92	Circular	20 (30)	Copper	0.027 – 4.35	0.1013	0°; 90°	Saturated
Iwamoto et al. [94]	128	Rectangular	18 × 10 (7.5), 18 × 18 (7.5), 18 × 40 (7.5), 18 × 76 (7.5)	Copper	Polished (roughness below 10	0.1013	0°; 90°	Saturated
	650	***Acceptable LHe datapoints***						
Liquid Hydrogen								
Class et al. [13]	45	Rectangular	25.4 × 558.8 (0.127)	Karma alloy	0.15 (smooth), 0.67 (rough)	0.0831 – 0.8511	0°; 90°	Saturated

(*continued on next page*)

Table 6 (*continued*)

Reference	Acceptable Nucleate Boiling Datapoints	Heater Geometry	Heater Size: Width x Length [mm^2] or Diameter (Thickness) [mm]	Heater Material	Surface roughness [μm]	Pressure [MPa]	Inclination Angle	Boiling State
Merte [73]	10	Circular	76.2	Copper	Polished 600 grit	0.1023 – 0.1027	0°; 90°	Saturated
Kozlov & Nozdrin [92]	35	Circular	30 (18, 12)	Stainless steel, aluminum alloy, copper	Not mentioned	0.0072 – 0.13	0°	Saturated
Shirai et al. [19]	156	Rectangular	10 × 100 (0.1)	Manganin	Not mentioned	0.11 – 1.0994	0°	Saturated, subcooled
	246	***Acceptable LH_2 datapoints***						
Liquid Oxygen								
Lyon et al. [67]	81	Flat ring	ID – 64.5 OD – 68.5 (0.0508)	Platinum	Not mentioned	0.0228 – 4.8484	0°	Saturated
Kosky [70]	210	Circular	19.05	Platinum	Polished	0.0226 - 4.9193	0°	Saturated
Ashworth et al.[a] [90]	16	Square	25.4 × 25.4 (5)	Aluminum	Smooth	0.1013	90°	Saturated
	307	***Acceptable LOX datapoints***						
Liquid Argon								
Kosky [74]	124	Circular	19.05	Platinum	Polished	0.0755 - 4.6201	0°	Saturated
Ashworth et al.[a] [94]	18	Square	25.4 × 25.4 (5)	Aluminum	Smooth	0.1013	90°	Saturated
	142	***Acceptable LAr datapoints***						
Liquid Methane								
Kosky [70]	69	Circular	19.05	Platinum	Polished	0.0347 - 4.1201	0°	Saturated
	69	***Acceptable LCh_4 datapoints***						
Parahydrogen								
Graham et al.[b] [66]	77	Rectangular ribbon	12.7 × 1.5875 (0.14224)	Chromel – A	Not mentioned	0.2930 – 0.6722	90°	Saturated
	77	***Acceptable parahydrogen datapoints***						
	2908	***Total acceptable data points***						

[a] Dimensions of the heater were measured from the heated surface figure.
[b] The Information of experimental apparatus was obtained from Baldwin et al. [104].

Fig. 10 shows predictions for the remaining Category 1 models and correlations yielding MAEs of 66.48 % or higher. It is obvious that aside from the correlation by Gross [56], all others exhibit significant deviations from the data. It is important to note that Gross's correlation is identical to that of Cooper [46] (which belongs to Category 2), except that Gross excludes Cooper's surface roughness term.

4.4. Assessment of category 2 models and correlations involving surface roughness parameter

As indicated earlier, Category 2 includes models and correlations that incorporate a surface roughness term, such as R_a or R_p, information that is available for only a subset of 437 data points of the Consolidated Database total of 2908 datapoints. Fig. 11 shows predictions for the Category 2 models and correlations by Danilova [53], Cooper [46], Ribatski and Jabardo [61], Kaminaga et al. [57], and Nishikawa et al. [38], which exhibit MAEs of 32.09 %, 36.55 %, 43.87 %, 54.73 %, and 64.97 %, respectively.

It must be noted that Danilova's correlation, which yields the best predictions in Category 2, lacks recommendations regarding a specific coefficient C. Therefore, a value of $C = 30$, was arrived at in the present study by trial and error in pursuit of lowest MAE. Similarly, Ribatski and Jabardo's correlation lacks recommendations for both C and exponent n of heat flux. A similar trial and error methodology was adopted in the present study, yielding the values of $C = 30$ and exponent $n = 0.72$. Additionally, it is important to note that roughness data are available for only three cryogens: LN_2, LHe, and LH_2, which compromises overall usefulness of Category 2 models and correlations compared to those of Category 1.

An intriguing analysis was undertaken to delve deeper into the effect of surface roughness wherein all models and correlations in Category 2 were reevaluated, this time by ignoring the term containing the surface roughness. This is identical to how Gross [56] recommended deleting the roughness term in Cooper's correlation [46] in pursuit of better predictions against data among majority of which roughness information is unavailable. Results of this exercise are captured in Fig. 12, which shows predictions for models and correlations for which the roughness term is ignored. Interestingly, the models and correlations by Danilova [53] and Ribatski and Jabardo [61] show very small increases in the MAE, while the models and correlations by Cooper [46], Nishikawa et al. [38], and Kaminaga et al. [57] all show better performance when the roughness term is ignored.

From this exercise, it is evident that inclusion of a roughness term in general does not improve the predictive accuracy of a model or correlation. This of course does not imply that surface roughness has no impact on the HTC. Rather, it highlights both the complexity of this effect and inadequacy of parameters commonly incorporated in certain prior models and correlations (e.g., R_a and R_p) in fully accounting for the roughness effect. In other words, additional roughness parameters are needed for a more complete characterization of the surface roughness. Unfortunately, a complete account of roughness parameters is absent even among models and correlations that attempt to incorporate the roughness effect. Another factor contributing to the uncertainty in accounting for surface roughness is absence of roughness information altogether from vast majority of available databases. This is especially the case for cryogenic data as evident from the present Consolidate Database, wherein only 437 datapoints of the total of 2908 datapoints include some (albeit incomplete) roughness parameter information. Additionally, datapoints for which certain roughness parameters are available belong to only three cryogens, LN_2, LHe, and LH_2, while no parameters are available for LAr, LOX, LCH_4, or parahydrogen.

These important facts guided our decision to exclude the use of surface roughness in the development of our new universal correlation while concurrently propose that any future cryogenic pool boiling

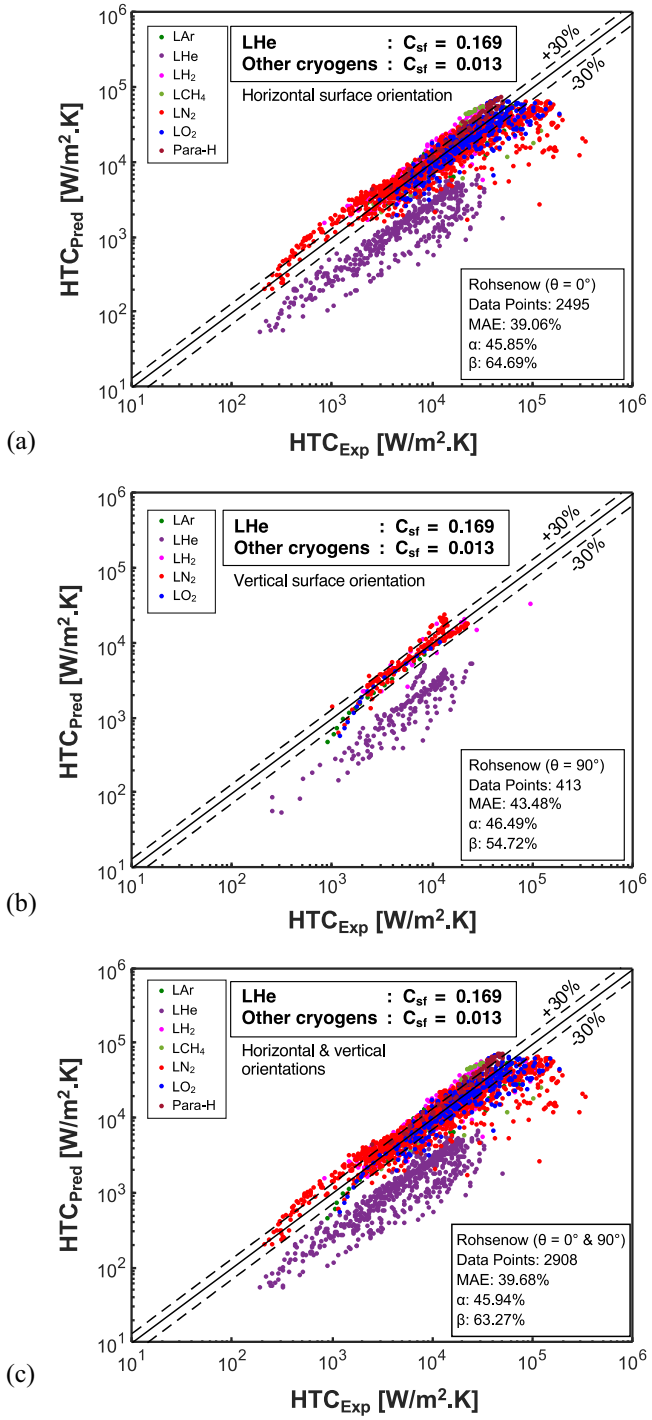

Fig. 6. Comparison of Rohsenow correlation's predictions for saturated nucleate pool boiling in terrestrial gravity and (a) horizontal, (b) vertical, and (c) combined orientations.

experiments must involve detailed account of roughness effect, including parameters other than only R_a or R_p since prior studies (e.g., Vachon et al. [11]) have shown inadequacy of these parameters at fully accounting for the surface roughness effects.

4.5. Category 3 models and correlations

As indicated earlier, only a small fraction of the prior models and correlations correctly account for effects of nucleation site density (N) and heating wall (e.g., material, thermal properties, size, shape, and

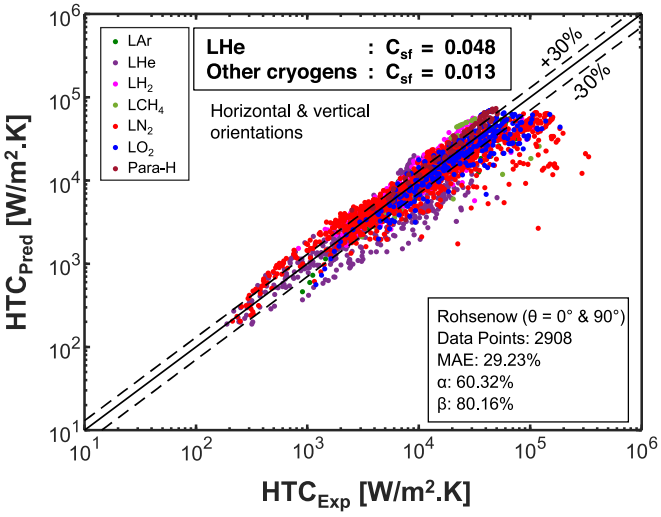

Fig. 7. Predictions using C_{sf} values of 0.048 for LHe and 0.013 for other cryogens, which yield best overall predictions for Rohsenow's correlation for saturated nucleate pool boiling in terrestrial gravity and horizontal and vertical orientations combined.

thickness); such information is mostly unavailable for cryogens in the Consolidated Database. This deficiency precludes ability to account for these important effects in developing a new HTC correlation. Nonetheless, for the sake of completeness, these correlations are included in Table 3.

4.6. Summary of statistical results of prior models and correlations

To provide a comprehensive overview in a single representation, overall statistical performances of the prior models and correlations are provided in Fig. 13. This figure showcases results for MAE and percentages of predictions falling within the ±30 % (α) and ±50 % (β) of the data. Better predictive accuracy is indicated by lower values of MAE and higher values of both α and β. Additional quantitative details are presented in Table 8. For the sake of comparison, results of our new correlation (to be presented below) are also included in both Fig. 13 and Table 8.

Table 7
C_{sf} values yielding least MAE for horizontal, vertical, and combined orientations.

Cryogen	No. of Data Points	C_{sf} for Least MAE
Horizontal and vertical orientations combined		
LHe	650	0.048
Para-H	77	0.017
LH_2	246	0.019
LN_2	1417	0.013
LO_2	307	0.012
LCH_4	69	0.019
LAr	142	0.013
Horizontal orientation only		
LHe	469	0.050
Para-H	77	0.017
LH_2	223	0.019
LN_2	1242	0.013
LO_2	291	0.012
LCH_4	69	0.019
LAr	124	0.013
Vertical orientation only		
LHe	181	0.044
Para-H	0	No data available
LH_2	23	0.013
LN_2	175	0.013
LO_2	16	0.012
LCH_4	0	No data available
LAr	18	0.011

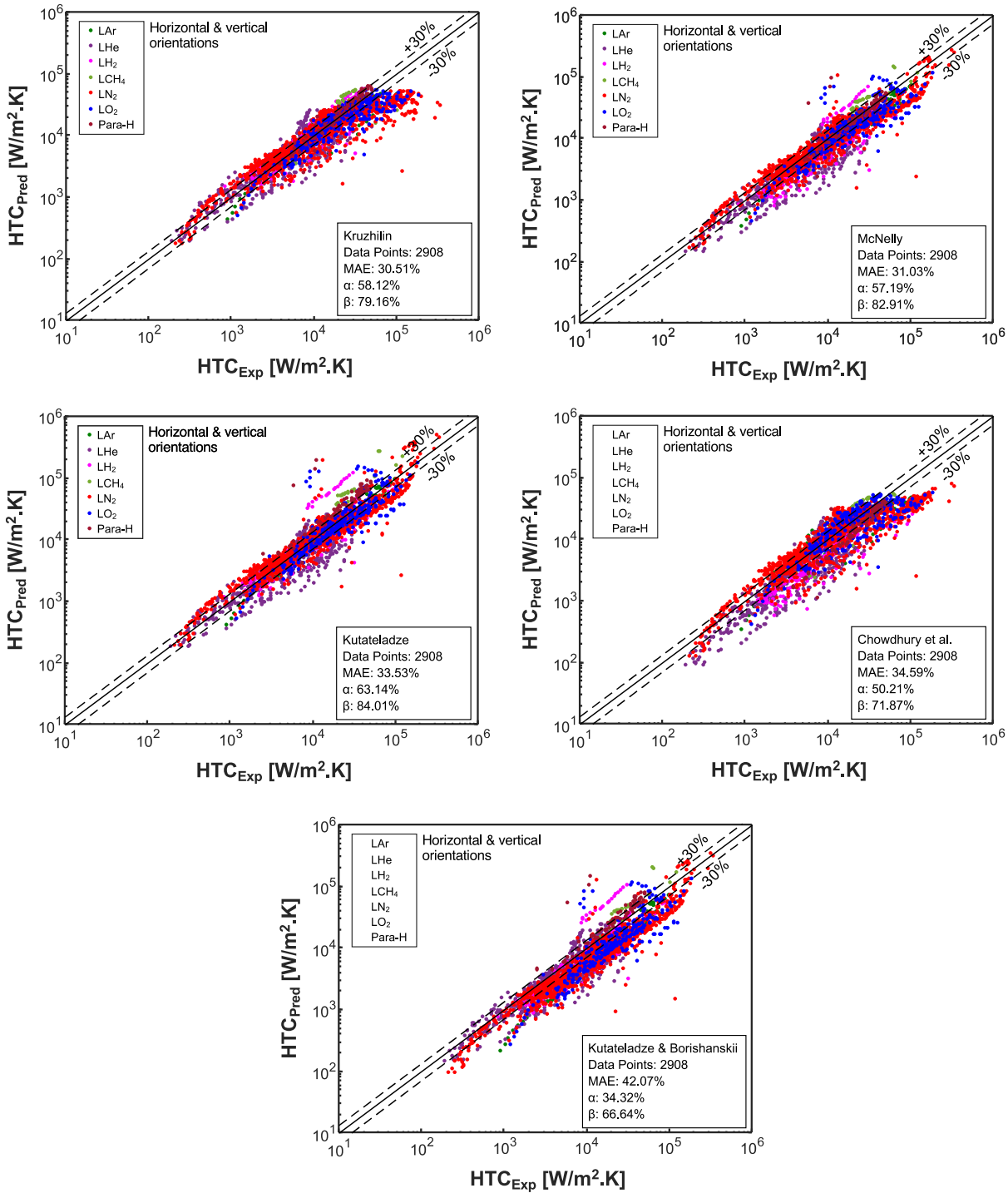

Fig. 8. Predictions of best performing Category 1 correlations for saturated nucleate pool boiling in terrestrial gravity and combined horizontal and vertical orientations.

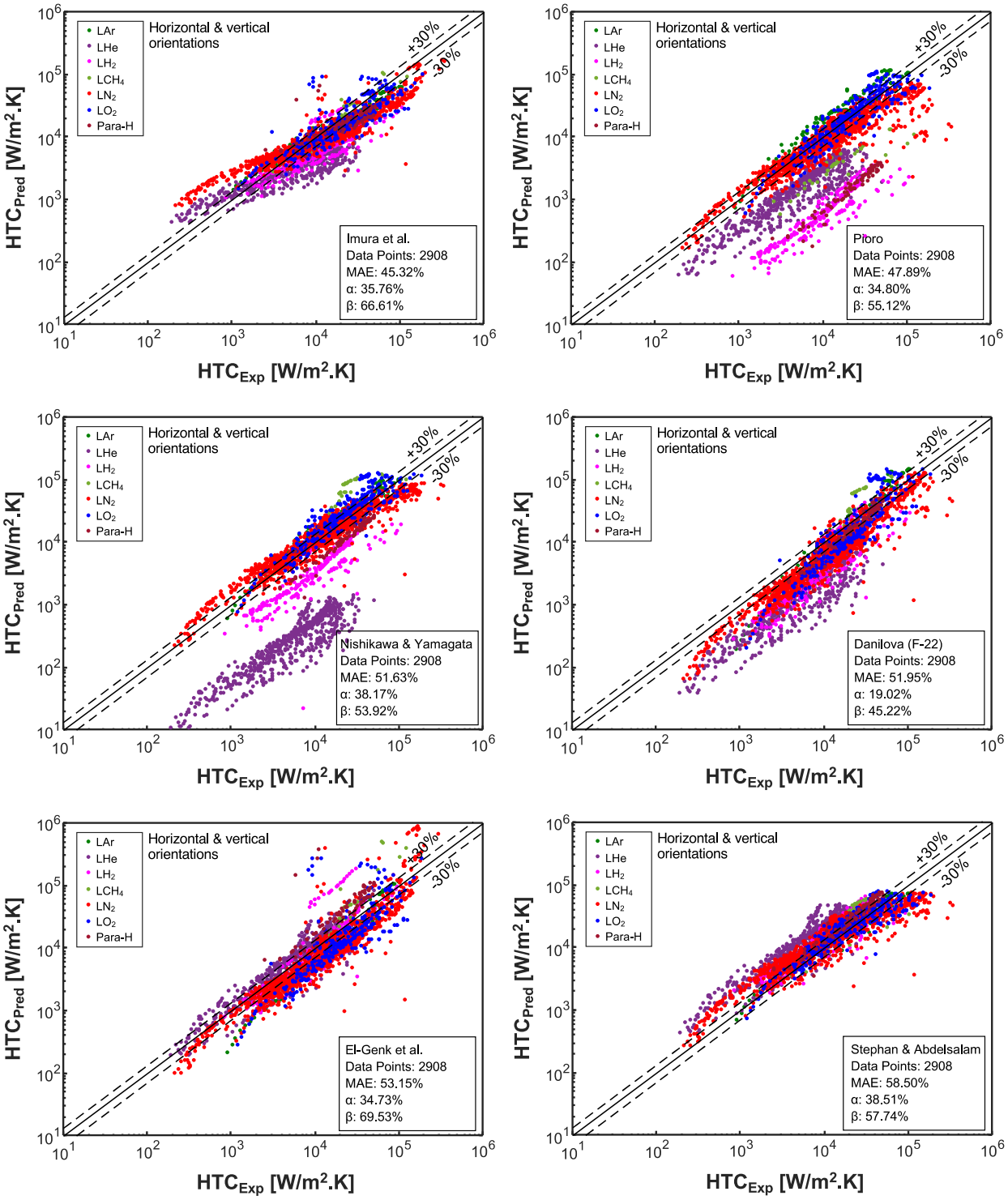

Fig. 9. Predictions of Category 1 correlations yielding intermediate accuracy for saturated nucleate pool boiling in terrestrial gravity and combined horizontal and vertical orientations.

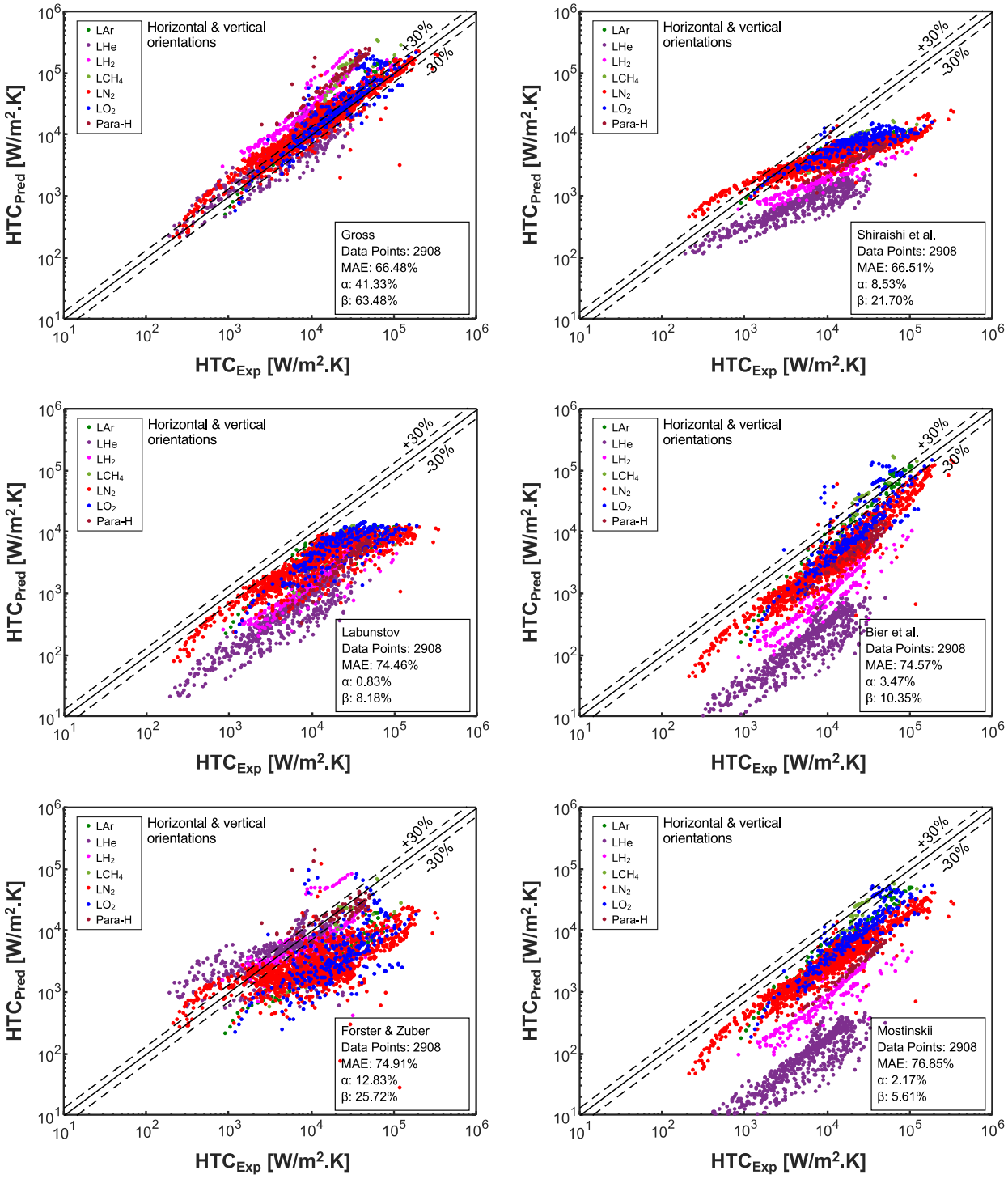

Fig. 10. Predictions of Category 1 correlations yielding lower accuracy for saturated nucleate pool boiling in terrestrial gravity and combined horizontal and vertical orientations.

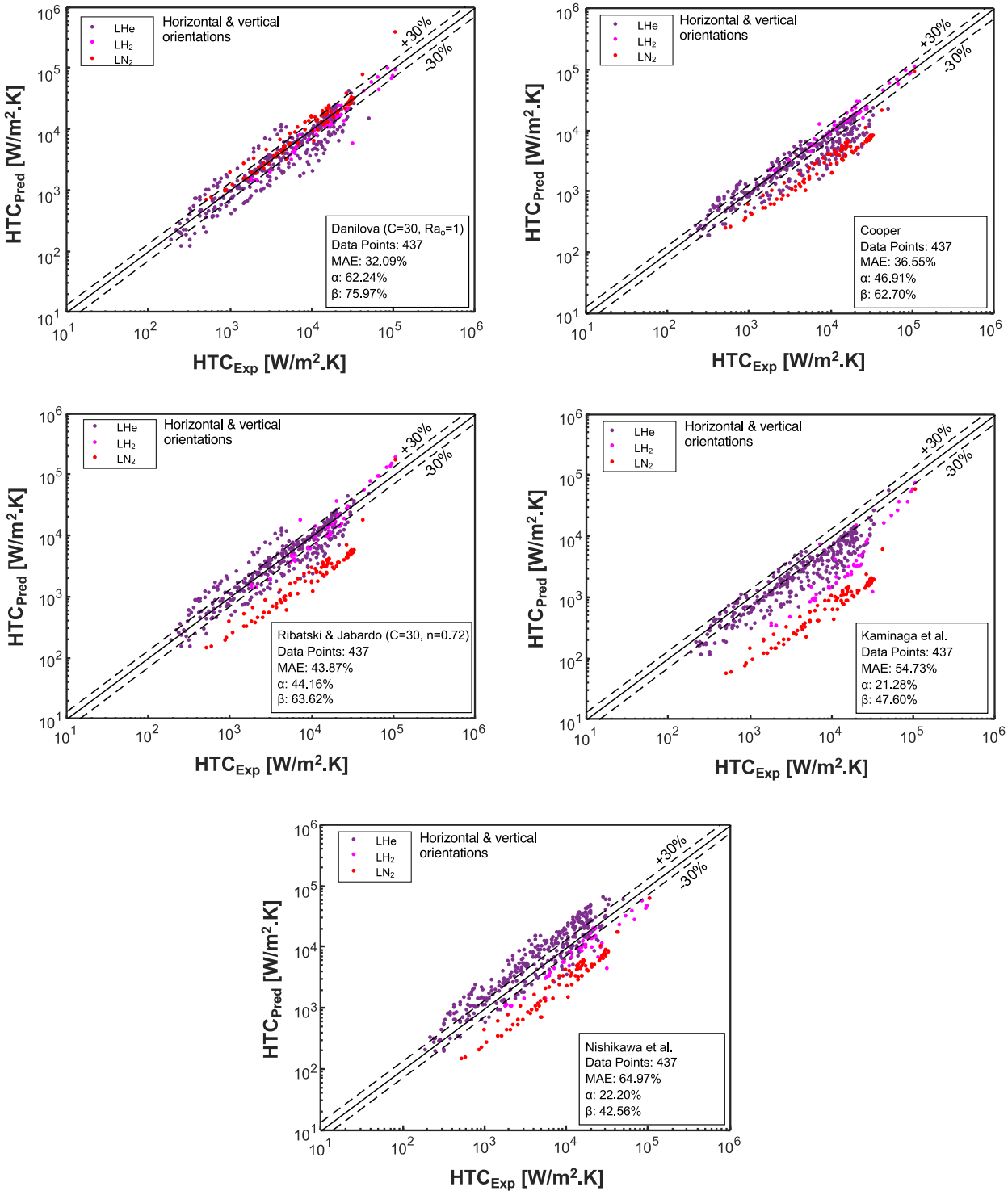

Fig. 11. Predictions of Category 2 correlations for saturated nucleate pool boiling in terrestrial gravity and combined horizontal and vertical orientations. Presented correlations include surface roughness effects.

5. New universal saturated pool boiling heat transfer correlation for cryogens

5.1. Parametric distribution of consolidated database and future recommendations

After the exclusion of certain data points based on the criteria presented in Section 3.1, the final Consolidated Database consists of 2908 data points encompassing seven cryogenic fluids: LAr, LHe, LH_2, LCH_4, LN_2, LO_2, and parahydrogen. Fig. 14 shows the distribution of vital parameters of the Consolidated Database in terms of number of datapoints versus year of publication, surface orientation angle, reduced pressure, system pressure, heat flux, and HTC.

The parametric distribution in Fig. 14, summary of consolidated database in Fig. 5, and earlier discussion on surface roughness effect serve as important guides to identifying crucial gaps in available cryogenic data. These gaps are the basis for the following recommendations for future experimental work:

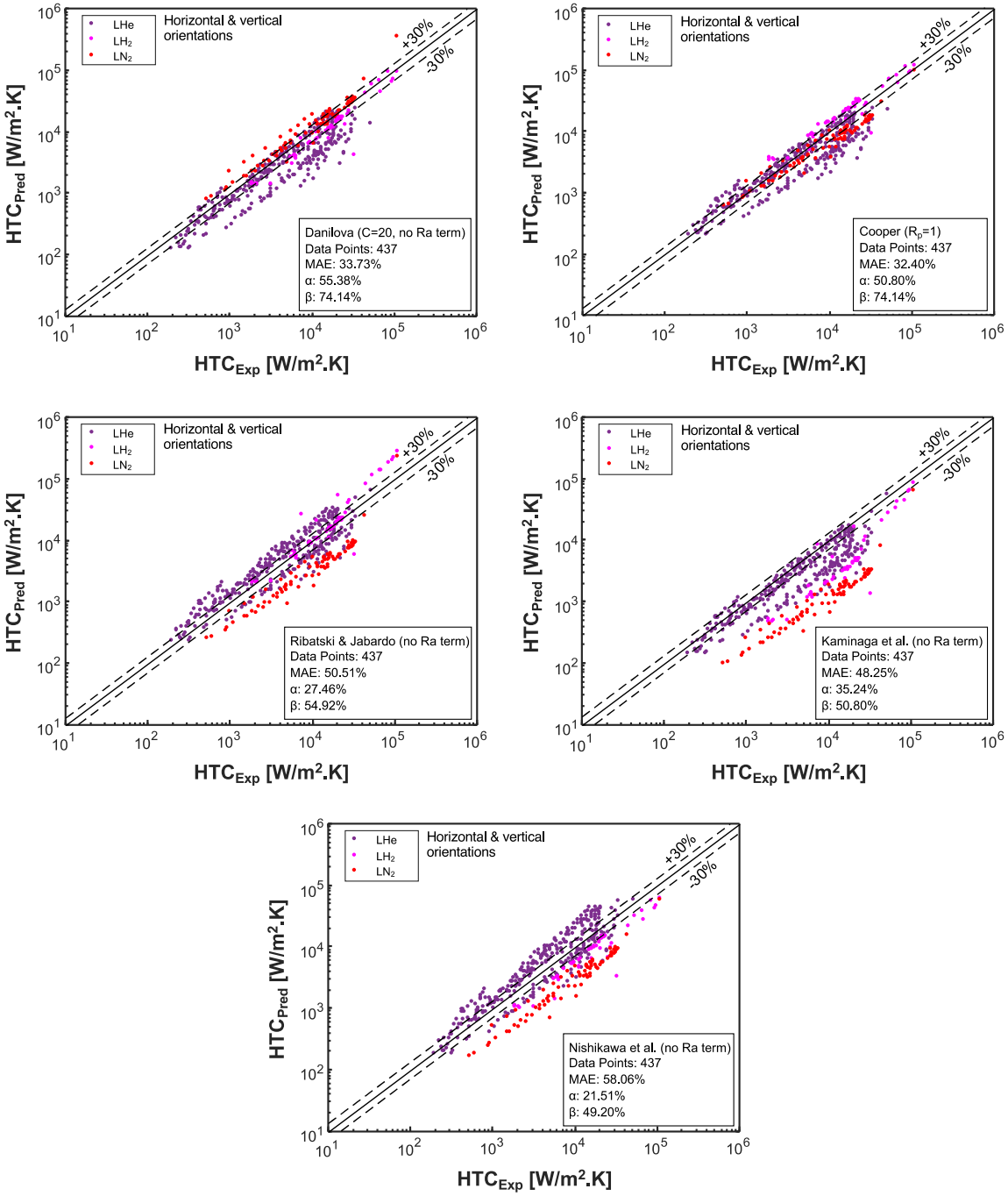

Fig. 12. Predictions of Category 2 correlations for saturated nucleate pool boiling in terrestrial gravity and combined horizontal and vertical orientations. Presented correlations exclude surface roughness effects.

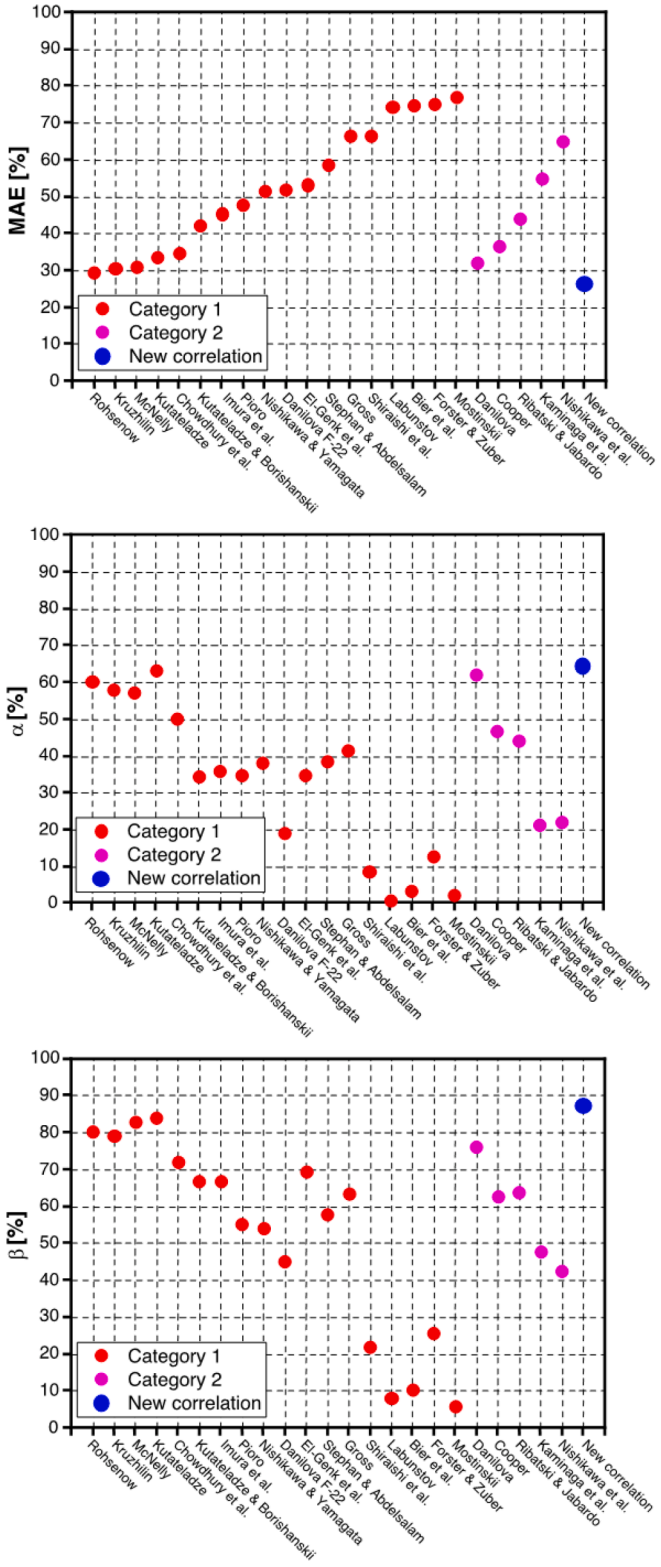

Fig. 13. Summary of predictive performances of all assessed correlations.

i. More work is needed to provide additional data for LAr, LCH_4, and parahydrogen.
ii. More data are needed to address effects of surface orientations other than horizontal.
iii. More attention in future experiments is needed to cover elevated pressures and high heat fluxes.

Table 8
Performance summary of all Category 1 and Category 2 models and correlations compared to that of the new correlation.

	Author(s)	MAE [%]	Data Within ±30 (α) [%]	Data Within ±50 (β) [%]	No. of data points
Category 1					
1	Rohsenow [32]	29.3	60.35	80.12	2908
2	Kruzhilin [29]	30.51	58.12	79.16	2908
3	McNelly [36]	31.03	57.19	82.91	2908
4	Kutateladze [31]	33.53	63.14	84.01	2908
5	Chowdhury et al. [58]	34.59	50.21	71.87	2908
6	Kutateladze & Borishanskiĭ [30]	42.07	34.32	66.64	2908
7	Imura et al. [45]	45.32	35.76	66.61	2908
8	Pioro [50]	47.89	34.80	55.12	2908
9	Nishikawa & Yamagata [56]	51.63	38.17	53.92	2908
10	Danilova [53]	51.95	19.02	45.22	2908
11	El-Genk et al. [65]	53.15	34.73	69.53	2908
12	Stephan & Abdelsalam [43]	58.50	38.51	57.74	2908
13	Gross [62]	66.48	41.33	63.48	2908
14	Shiraishi et al. [44]	66.51	8.53	21.70	2908
15	Labunstov [42]	74.46	0.83	8.18	2908
16	Bier [60]	74.57	3.47	10.35	2908
17	Forster & Zuber [37]	74.91	12.83	25.72	2908
18	Mostinskii [57]	76.85	2.17	5.61	2908
Category 2					
19	Danilova [53]	32.09	62.24	75.97	437
20	Cooper [46]	36.55	46.91	62.70	437
21	Ribatski & Jabardo [61]	43.87	44.16	63.62	437
22	Kaminaga et al. [57]	54.73	21.28	47.60	437
23	Nishikawa et al. [38]	64.97	22.20	42.56	437
New Correlation					
24		**25.36**	**64.48**	**87.24**	**2908**

iv. As indicated earlier, vital surface roughness information is very limited in prior studies, which warrants especial attention in future experiments.
v. Focus needs to be devoted to capture new data in both microgravity and both Lunar and Martian gravities. Thereafter, gravity scaling analysis should be applied to the prior correlations as well as the new correlation, as done by Raj et al. [109] for non-cryogens and Wang et al. [110] for LH_2.
vi. Overall, attention should be given to providing from experiment *all the information required for correlating data*, including pressure, surface orientation, heat flux, wall temperature, HTC, heating wall (material, thermal properties, size, shape, and thickness), and, of course, surface roughness.

5.2. Development of new correlation for cryogens

With its substantial volume of datapoints, the Consolidated Database, despite the afore-mentioned gaps, will serve as basis for developing a new correlation for cryogenic nucleate pool boiling HTC that is both robust and universally applicable to all cryogenic fluids. Given the gaps detailed in earlier sections, the new correlation is formulated through reliance on the following premises:

i. Incorporation of data containing surface roughness information is deliberately avoided from analysis. This decision is based on the small percentage of datapoints with surface roughness information, inadequacy of complete surface roughness information from virtually all available data (including those for which some information is available), and absence of any surface roughness

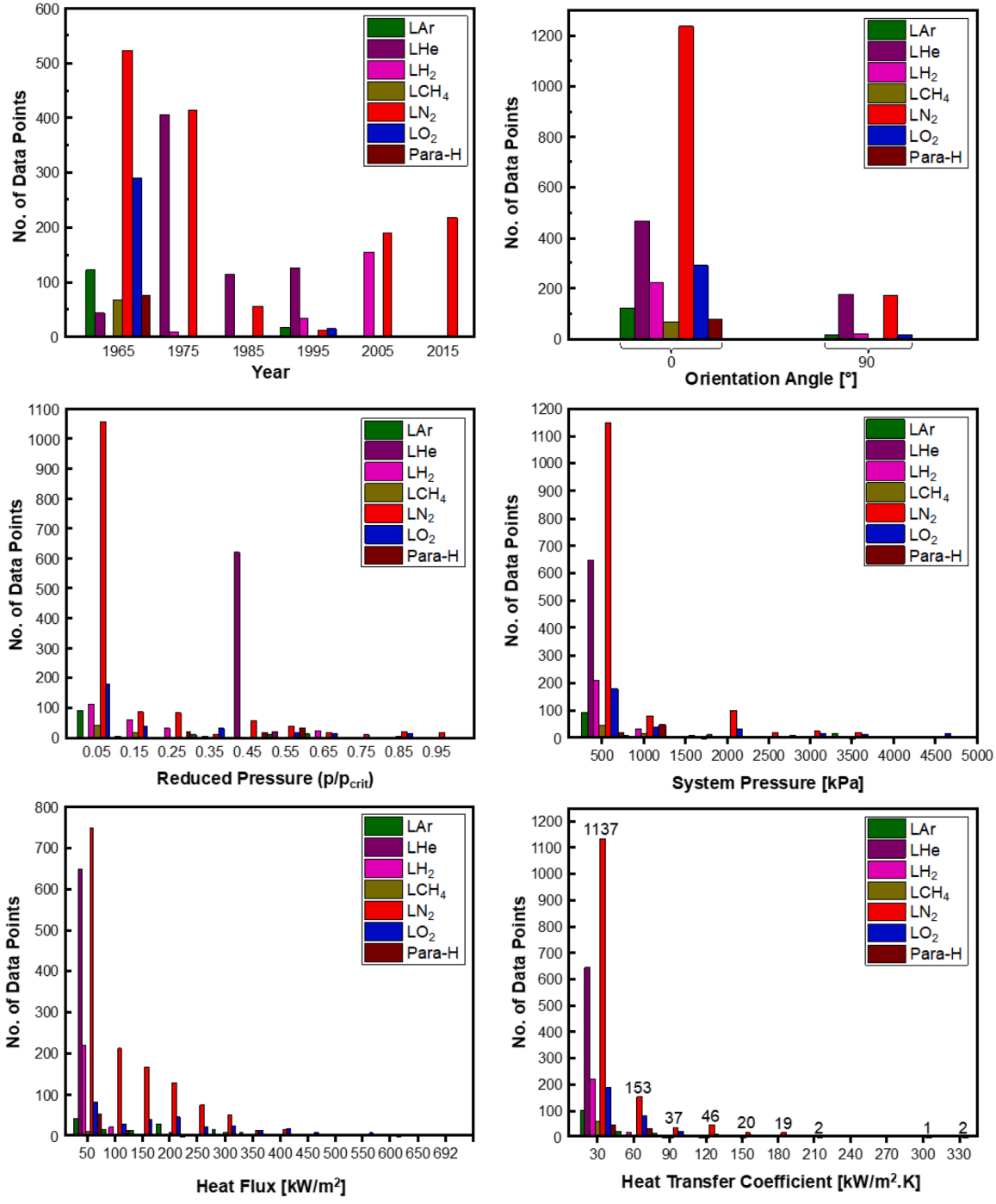

Fig. 14. Parametric distribution of consolidated database.

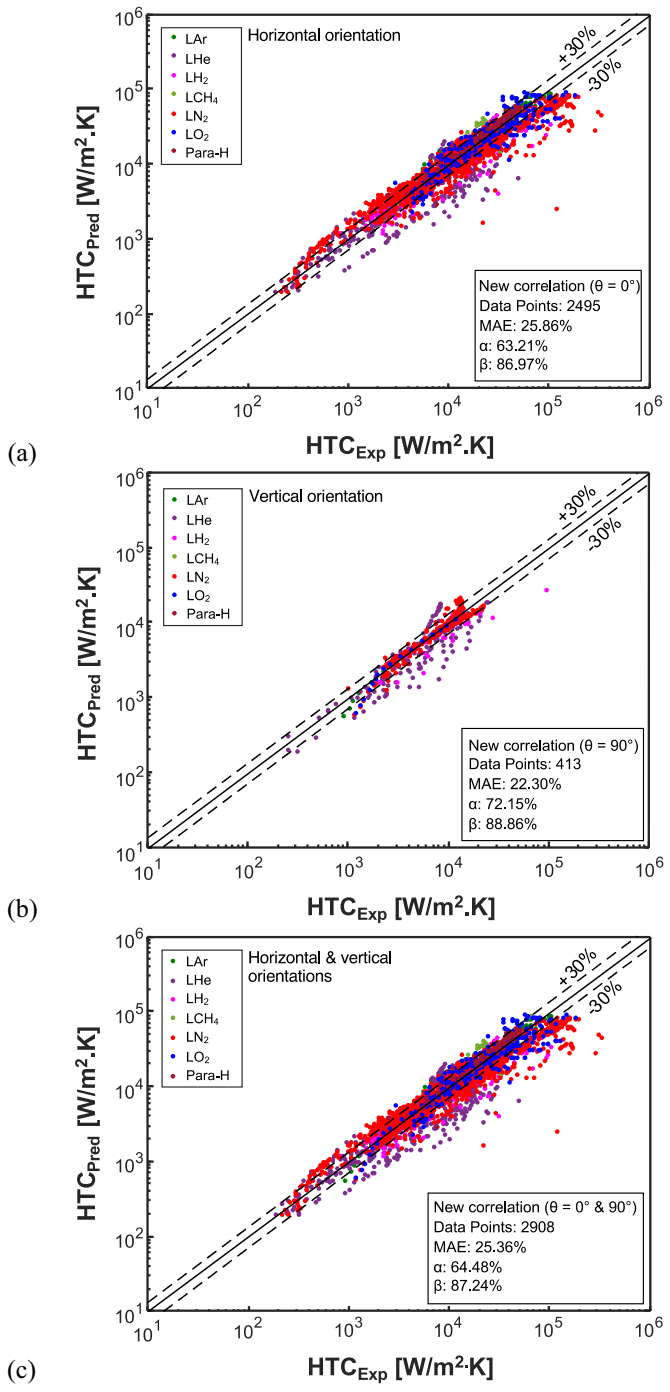

Fig. 15. Comparison of new correlation's predictions for saturated nucleate pool boiling in terrestrial gravity and (a) horizontal, (b) vertical, and (c) combined orientations.

information for LAr, LOX, LCH_4, and parahydrogen. This decision by no means diminishes the importance of surface roughness impact on HTC, which the present authors prescribe for all future experimental work.

ii. Incorporation of orientation angle is purposely avoided because of scarcity of data for orientations other than horizontal and to a lesser extent vertical, as well as non-monotonic influence of the orientation angle on the HTC. It should be noted that the HTC correlation sought in the present study is based on data for only horizontal and vertical surfaces.

iii. Use of the heating surface characteristics (material, thermal properties, size, shape, and thickness) is purposely avoided due to the prevalent absence of this information from most studies. Here too, the decision to avoid incorporating the surface characteristics by no means diminishes the importance of their influence on HTC, which the present authors prescribe for all future experimental work.

One important observation is that the vast majority of prior models and correlations consistently include three primary parameters: Pressure, heat flux, and liquid Prandtl number, information of which is also available for most data in the Consolidated Database. Therefore, those same parameters will be foundational for development of the new HTC correlation. However, it is important to acknowledge that, because of limited data for elevated pressures and high fluxes, accurately accounting for these extreme operating conditions is quite challenging. This issue will be addressed in Section 5.4.

Furthermore, upon meticulous examination, it became apparent that older models and correlations were typically grounded in mechanistic formulations that incorporated a variety of thermophysical properties. However, a significant shift in this trend occurred after 1963 (e.g., Mostinskii [52]) when many opted to replace individual thermophysical properties with pressure alone, given that in saturated nucleate pool boiling values of all thermophysical properties are inherently dictated by saturation pressure. To accommodate different fluids, investigators introduced parameters such as reduced pressure, critical pressure, and occasionally molecular weight of the fluid.

Taking into consideration the afore-mentioned insights, a new universal correlation for cryogens is formulated which employs three key parameters: heat flux, reduced pressure, and liquid Prandtl number. A functional form of the reduced pressure term was initially adopted from the Danilova's correlation [53], which subsequently underwent adjustments through extensive regression analysis to align with the Consolidated Database. Given the suboptimal performance of prior correlations for elevated pressures and high heat fluxes, a corrective multiplier is prescribed to tackle those extreme conditions. Determination of exponents and coefficients in the new correlation was determined by regression analysis facilitated via a custom Python program. Following is the final form for the new correlation for HTC:

$$h_{nb} = 13.3\, q''^{0.665}(1 + 0.52\, p^*)^{4.7} Pr_f^{-1.09}\left[\frac{1 + 68e^{20(p^*-1.1)}}{1 + 0.0045\, e^{(q''\times\ 10^{-5})}}\right] \quad (3)$$

where h_{nb} is the nucleate boiling HTC [W/m^2.K], p^* represents the reduced pressure (p/p_{crit}), q'' is the heat flux [W/m^2], and Pr_f denotes the Prandtl number of saturated liquid at the system pressure.

Predictions of the new correlation are shown in Fig. 15 for horizontal orientation, vertical orientation, and both orientations combined. The new correlation features an overall MAE of 25.36 %, with 64.48 % and 87.24 % of predictions falling within ±30 % and ±50 % of the data, surpassing the performances of all prior models and correlations. Notice that because the Consolidated Database primarily consists of horizontal data, the MAE for horizontal orientation (25.86 %) closely aligns with that for the combined orientations. However, the MAE for the vertical orientation is about 3 % lower than those for horizontal and combined orientations.

To demonstrate the new correlation's performance across the different cryogens independently, a detailed comparison is presented in Fig. 16. The new correlation is shown performing best for parahydrogen, with an MAE of 13.04 %, followed by LAr (20.55 %), LH_2 (21.45 %), LOX (23.18 %), LN_2 (26.32 %), LHe (27.61 %), and LCH_4 (31.51 %). The ability of the correlation to yield good predictions across the different cryogens is the basis for its designation as *universal correlation*.

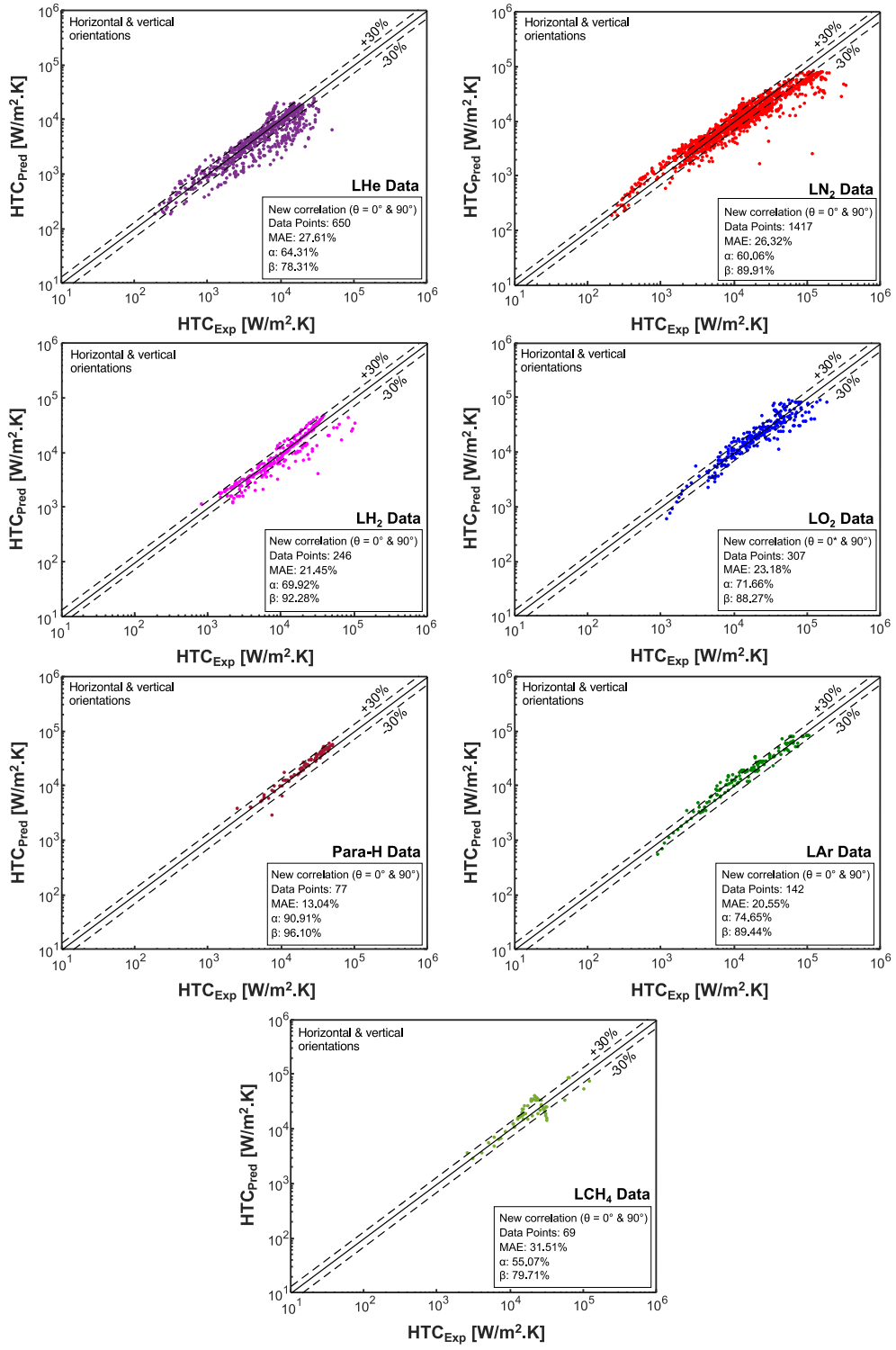

Fig. 16. Comparison of new correlation's predictions for saturated nucleate pool boiling in terrestrial gravity and combined orientations for individual cryogens.

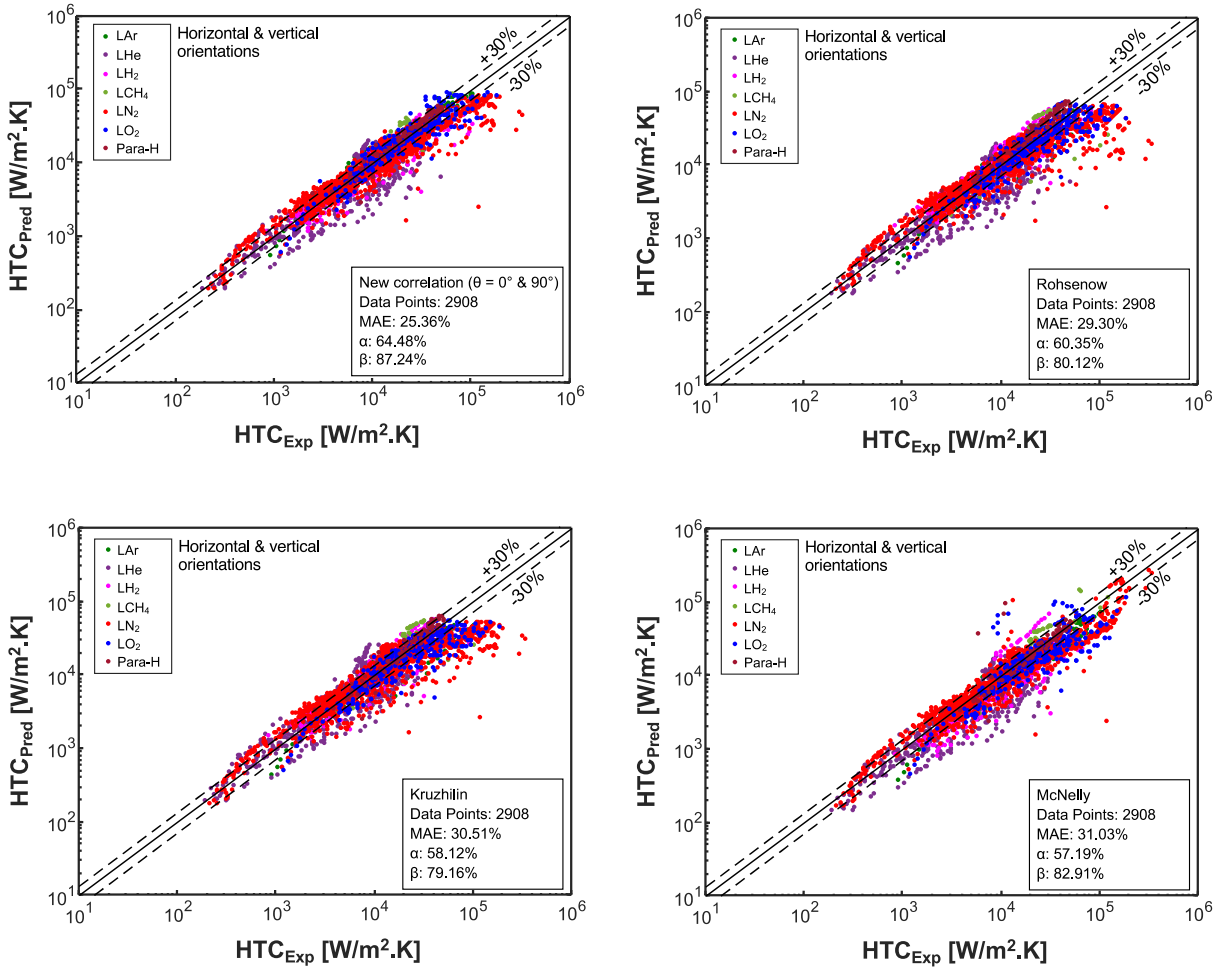

Fig. 17. Comparison of new correlation's predictions against those of best performing prior correlations for saturated nucleate pool boiling in terrestrial gravity and combined orientations.

5.3. Comparison of new correlation with prior best performing models and correlations

To demonstrate the superiority of the new correlation over existing ones, a thorough comparison is conducted against the three best performing prior models and correlations: Rohsenow [32], Kruzhilin [29], and McNelly [36]. The results of this comparative analysis are showcased in Fig. 17. Aside from lowest MAE of 25.36 %, the new correlation is also shown outperforming the other models and correlations in terms of the number of datapoints predicted within ±30 % and ±50 % of the data.

5.4. Advantages of new correlation over prior models and correlations in predicting elevated pressure and high heat flux data

Aside from attaining the lowest MAE, the new correlation (i) is deemed universal via ability to achieve good predictions across all cryogenic fluids of interest, and (ii) features rather simple formulation, relying on only three parameters: reduced pressure, heat flux, and liquid Prandtl number.

Through meticulous examination, it became apparent that the previous models and correlations yield notably high MAEs when applied to high-pressure data. Consequently, formulation of the new correlation, Eq. (3), has been fine-tuned specifically to tackle high-pressure data in the range of $p^* > 0.5$. Fig. 18 compares performance results for this pressure range, showing superiority of the new correlation, evidenced by lowest MAE of 35.29 %, followed by those of Rohsenow (49.48 %), McNelly (56.19 %), and Kruzhilin (57.15 %).

Like the difficulty predicting high pressure data, analysis shows prior models and correlations also yield poor predictions against high flux data surpassing 300 kW/m^2. Here too, a multiplier has been incorporated in the new correlation to tackle the high heat flux data. Fig. 19 compares predictions for the high heat flux range, showcasing superior performance of the new correlation, having the lowest MAE of 26.56 %, followed by those of Rohsenow (36.81 %), McNelly (35.23 %), and Kruzhilin (39.79 %).

6. Conclusions

The motivation behind this study stems from the absence of a substantial and dependable nucleate pool boiling database for cryogenic fluids. This database is crucial for evaluating the predictive accuracy of existing models and correlations, as well as to develop a new, improved predictive method. To fulfill this purpose, a Consolidated Cryogenic Nucleate Pool Boiling Database comprising heat transfer coefficients (HTCs) for flat surfaces was meticulously assembled from a comprehensive review of global literature. Following are key findings from this study:

1. A comprehensive investigation of the mechanisms and prevailing trends in nucleate pool boiling has been undertaken. The impact of various parameters on the HTC in nucleate pool boiling has been succinctly summarized. A compilation of 30 distinct models and correlations was presented for evaluation of predictive accuracy.

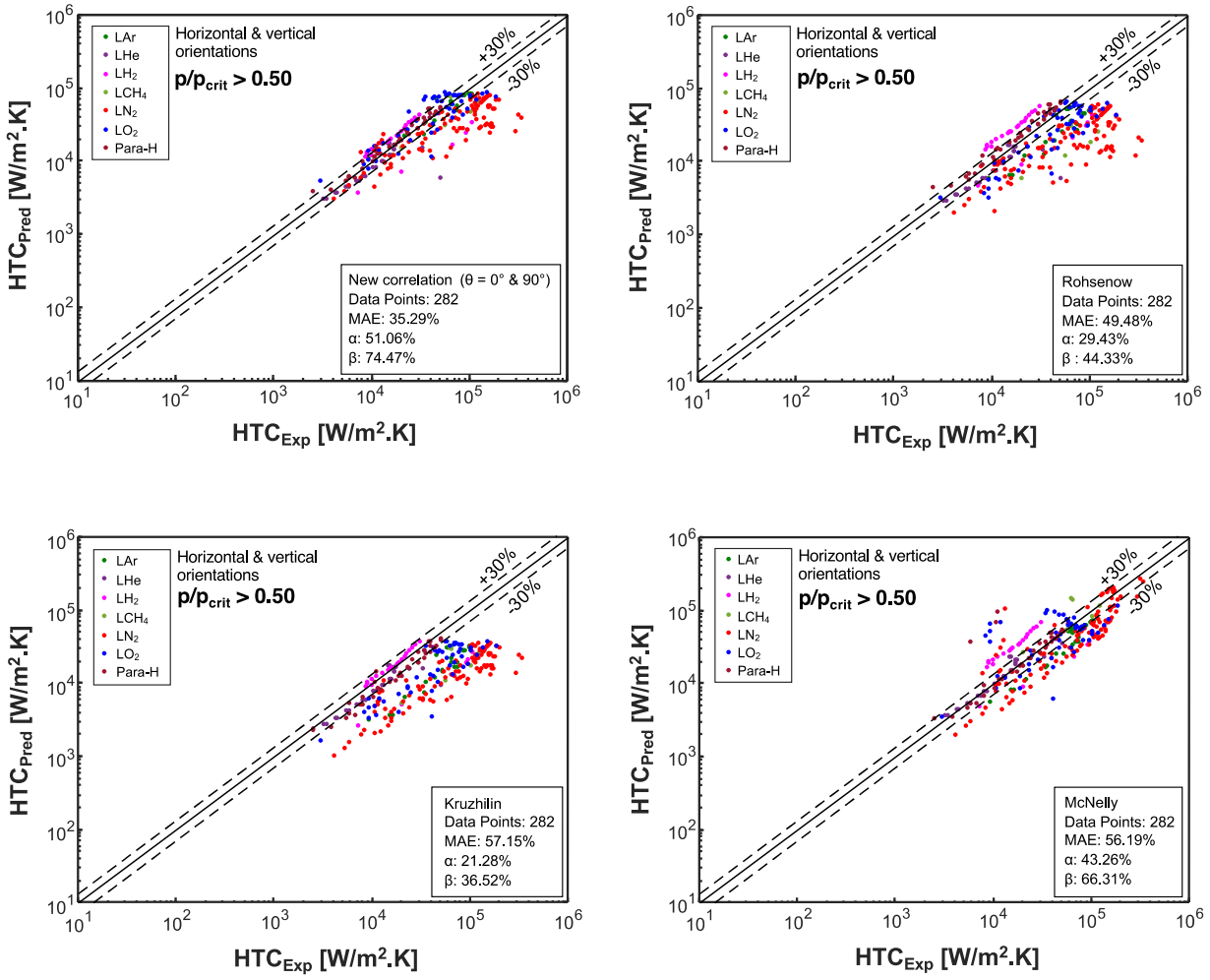

Fig. 18. Comparison of new correlation's predictions against those of best performing prior correlations for saturated nucleate pool boiling in terrestrial gravity, combined orientations, and elevated pressure data ($p/p_{crit} > 0.50$).

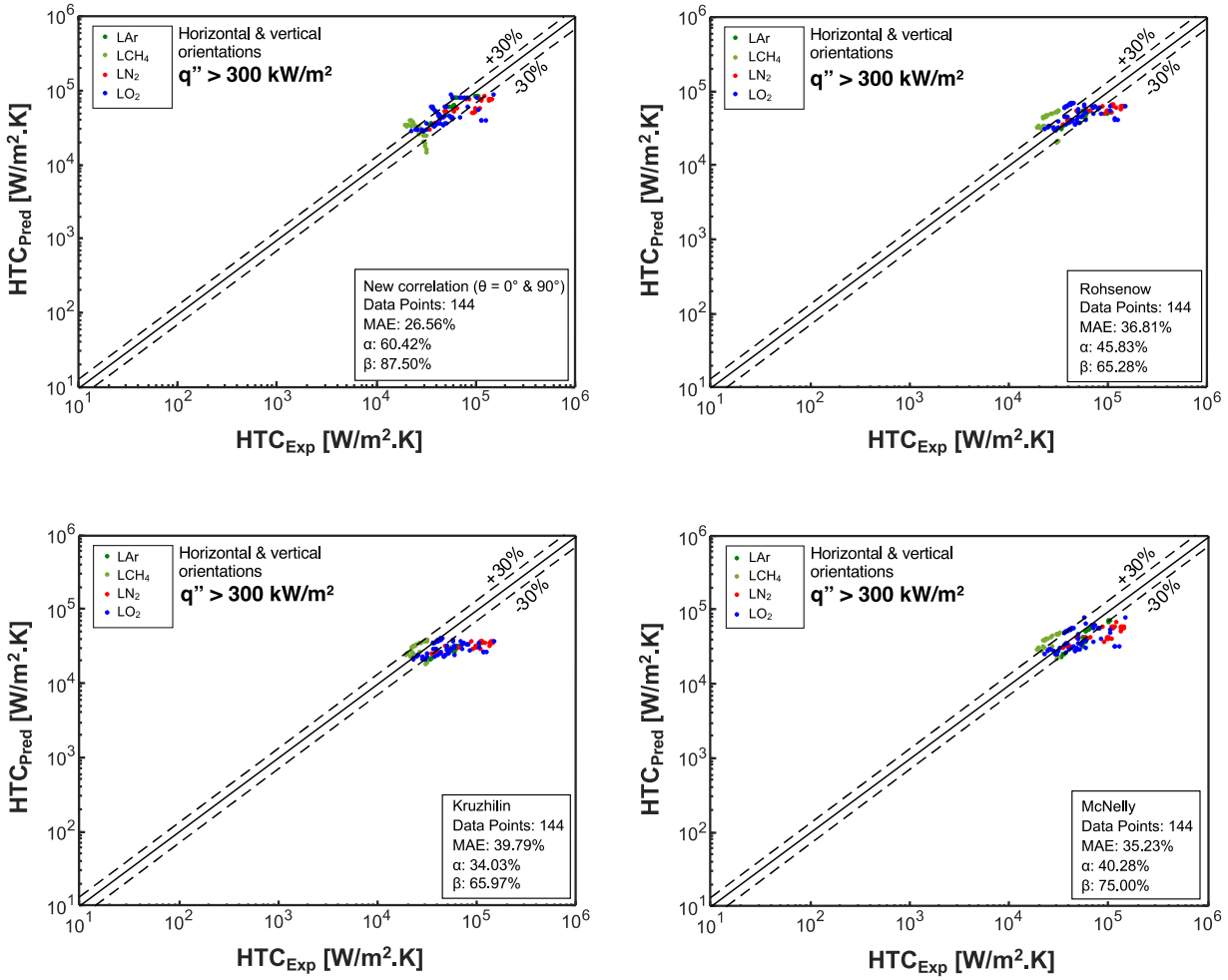

Fig. 19. Comparison of new correlation's predictions against those of best performing prior correlations for saturated nucleate pool boiling in terrestrial gravity, combined orientations, and high flux data (q" > 300 kW/m^2).

2. Stringent criteria were adopted to assemble the Consolidated Database, which culminated in 2908 nucleate pool boiling data points collected from 48 references and encompass seven cryogenic fluids: LHe, LN_2, LH_2, LOX, LAr, LCH_4, and parahydrogen. Notably, a significant majority (85.8 %) of the datapoints are for the horizontal upward-facing orientation ($\theta = 0^\circ$), while the remaining 14.2 % correspond to the vertical orientation ($\theta = 90^\circ$).
3. A detailed evaluation of prior models and correlations was conducted, revealing a broad range of accuracies. These predictive tools were segregated into three categories. The first includes formulations based on parameters that are fully prescribed in the Consolidated Database. The second group consists of models and correlations wherein certain parameters are missing from most of the Consolidated Database, such as surface roughness. The third group includes models and correlations that involve specific parameters for which no data are currently available.
4. During the evaluation of prior predictive tools, special attention was devoted to the Rohsenow correlation [32], given its unmatched popularity in both research articles and textbooks. The Consolidated Database enabled determination of optimal values for a key parameter, C_{sf}, in this correlation for cryogens. Using a C_{sf} value of 0.048 for liquid helium and 0.013 for all other cryogens yielded a MAE of 29.3 %.
5. The Consolidated Database enabled the formulation of a new, and simple correlation for cryogenic HTC for nucleate boiling from horizontal and vertical flat surfaces that is based on only three parameters: pressure, heat flux, and liquid Prandtl number. This correlation outperformed all prior models and correlations in the literature, supported by a MAE of 25.36 % with 64.48 % and 87.24 % of predictions falling within ±30 % and ±50 % of the data, respectively.
6. Despite the success of the new correlations, it is recommended that future experiments be conducted to fill in major gaps in the available cryogenic databases. Key among future endeavors will be the detailed characterization of all crucial surface roughness parameters, and acquisition of comprehensive databases for multiple surface orientations, elevated pressures, and high fluxes. Additionally, while the present study was focused entirely on 1-g_e conditions, a long-term objective will be to extend the work to reduced gravity conditions, including microgravity and both Lunar and Martian gravities.

CRediT authorship contribution statement

Faraz Ahmad: Writing – original draft, Validation, Software, Methodology, Investigation, Formal analysis, Data curation, Conceptualization. **Sunjae Kim:** Methodology, Formal analysis. **Michael Meyer:** Writing – review & editing, Supervision, Methodology, Formal analysis. **Jason Hartwig:** Writing – review & editing, Supervision, Project administration, Methodology, Investigation, Funding acquisition, Conceptualization. **Issam Mudawar:** Writing – review & editing, Writing – original draft, Validation, Supervision, Project administration, Methodology, Investigation, Funding acquisition, Formal analysis, Conceptualization.

Declaration of competing interest

The authors declare the following financial interests/personal relationships which may be considered as potential competing interests: Issam Mudawar reports financial support was provided by NASA. If there are other authors, they declare that they have no known competing financial interests or personal relationships that could have appeared to influence the work reported in this paper.

Data availability

The data that has been used is confidential.

Acknowledgment

The authors are grateful for financial support of the National Aeronautics and Space Administration (NASA) Small Business Technology Transfer (STTR) program under a subcontract from MTS Inc. Phase II contract 80NSSC23CA009. We also thank the Fulbright Program for providing a scholarship for the first author.

References

[1] V. Ganesan, R. Patel, J. Hartwig, I. Mudawar, Review of databases and correlations for saturated flow boiling heat transfer coefficient for cryogens in uniformly heated tubes, and development of new consolidated database and universal correlations, Int. J. Heat Mass Transf. 179 (2021) 121656.
[2] E.W. Lemmon, I.H. Bell, M.L. Huber, M.O. McLinden, NIST standard reference database 23: reference fluid thermodynamic and transport properties-REFPROP, Version 10.0, Gaithersburg, MD (2018).
[3] J. Kim, Review of nucleate pool boiling bubble heat transfer mechanisms, Int. J. Multip. Flow 35 (2009) 1067–1076.
[4] P.J. Marto, J.A. Moulson, M.D. Maynard, Nucleate pool boiling of nitrogen with different surface conditions, J. Heat Transf. 90 (1968) 437–444.
[5] W.M. Rohsenow, P. Griffith, Correlation of Maximum Heat Flux Data For Boiling of Saturated Liquids, Heat Transfer Lab., Massachusetts Institute of Technology, 1955. Tech report.
[6] W.M. Rohsenow, J.A. Clark, A study of the mechanism of boiling heat transfer, Trans. ASME 73 (1951) 609–616.
[7] K. Engelberg-Forster, R. Greif, Heat transfer to a boiling liquid—Mechanism and correlations, J. Heat Transf. 81 (1959) 43–52.
[8] R.F. Gaertner, Photographic study of nucleate pool boiling on a horizontal surface, J. Heat Transf. 87 (1965) 17–27.
[9] D.V. Porchey, Ph.D. thesis, University of Missouri – Rolla, 1970.
[10] Y.Y. Hsu, On the size range of active nucleation cavities on a heating surface, J. Heat Transf. 84 (1963) 207–216.
[11] R.I. Vachon, G.E. Tanger, D.L. Davis, G.H. Nix, Pool boiling on polished and chemically etched stainless-steel surfaces, J. Heat Transf. 90 (1968) 231–238.
[12] I.L. Pioro, W. Rohsenow, S.S. Doerffer, Nucleate pool-boiling heat transfer. I: review of parametric effects of boiling surface, Int. J. Heat Mass Transf. 47 (2004) 5033–5044.
[13] C.R. Class, J.R. DeHaan, M. Piccone, R.B. Cost, Boiling heat transfer to liquid hydrogen from flat surfaces, in: Advances in Cryogenic Engineering, Proc. 1959 Cryogenic Eng. Conf., Berkeley, CA, 1959.
[14] C. Bombardieri, C. Manfletti, Influence of wall material on nucleate pool boiling of liquid nitrogen, Int. J. Heat Mass Transf. 94 (2016) 1–8.
[15] S. Jun, J. Kim, S.M. You, H.Y. Kim, Effect of subcooling on pool boiling of water from sintered copper microporous coating at different orientations, Sci. Technol. Nucl. Install. (2018) 8623985.
[16] L. Lee, B.N. Singh, The influence of subcooling on nucleate pool boiling heat transfer, Lett. Heat Mass Transf. 2 (1975) 315–323.
[17] A.A. Watwe, A. Bar-Cohen, A. McNeil, Combined pressure and subcooling effects on pool boiling from a PPGA chip package, J. Electron. Packag. 119 (1997) 95–105.
[18] B.J. Suroto, M. Kohno, Y. Takata, Surface wettability and subcooling on nucleate pool boiling heat transfer, AIP Conf. Proc., 2018.
[19] Y. Shirai, H. Tatsumoto, M. Shiotsu, K. Hata, H. Kobayashi, Y. Naruo, Y. Inatani, Boiling heat transfer from a horizontal flat plate in a pool of liquid hydrogen, Cryogenics 50 (2010) 410–416.
[20] C. Zhang, L. Zhang, H. Xu, The influence of surface orientation on the onset of nucleate boiling from microporous surfaces, Int. J. Heat Fluid Flow 73 (2018) 163–173.
[21] A.H. Howard, I. Mudawar, Orientation effects on pool boiling critical heat flux (CHF) and modeling of CHF for near-vertical surfaces, Int. J. Heat Mass Transf. 42 (1999) 1665–1688.
[22] A. Priarone, Effect of surface orientation on nucleate boiling and critical heat flux of dielectric fluids, Int. J. Therm. Sci. 44 (2005) 822–831.
[23] K.N. Rainey, S.M. You, Effects of heater size and orientation on pool boiling heat transfer from microporous coated surfaces, Int. J. Heat Mass Transf. 44 (2001) 2589–2599.
[24] F.D. Akhmedov, V.A. Grigorev, A.S. Dudkevic, Boiling of nitrogen at pressures from atmospheric to critical, Therm. Eng. 21 (1974) 120–121.
[25] L. Bewilogua, R. Knöner, H. Vinzelberg, Heat transfer in cryogenic liquids under pressure, Cryogenics 15 (1975) 121–125.
[26] V.I. Deev, V.E. Keilin, I.A. Kovalev, A.K. Kondratenko, V.I. Petrovichev, Nucleate and film pool boiling heat transfer to saturated liquid helium, Cryogenics 17 (1977) 557–562.
[27] S.S. Kutateladze, Osnovy Teorii Teploobmena (Fundamentals of Heat Transfer Theory), Nauka, Novosibirsk, 1970.
[28] R. Patel, M. Meyer, J. Hartwig, I. Mudawar, Review of cryogenic pool boiling critical heat flux databases, Assessment of models and correlations, and development of new universal correlations, Int. J. Heat Mass Transf. 190 (2022) 122579.
[29] G.N. Kruzhilin, Free-convection transfer of heat from a horizontal plate and boiling liquid, Proc. USSR Academy of Sciences 58 (1947) 1657–1660.
[30] S.S. Kutateladze, V.M. Borishanskiĭ, A Concise Encyclopedia of Heat Transfer, Pergamon, 1966.
[31] S.S. Kutateladze, Heat Transfer and Hydrodynamic Resistance, 367, Energoatomizdat, Moscow, 1990.
[32] W.M. Rohsenow, A method of correlating heat-transfer data for surface boiling of liquids, Trans. ASME 74 (1952) 969–975.
[33] W.M. Rohsenow, J.P. Hartnett, Y.I. Cho, Handbook of Heat Transfer, McGraw-Hill New York, 1998.
[34] I.L. Pioro, Experimental evaluation of constants for the Rohsenow pool boiling correlation, Int. J. Heat Mass Transf. 42 (1999) 2003–2013.
[35] S.K. Das, D. Chatterjee, Vapor Liquid Two Phase Flow and Phase Change, Springer, 2023.
[36] M.J. McNelly, A correlation of rates of heat transfer to nucleate boiling of liquids, J. Imperial College Chem. Eng. Soc. 7 (1953) 18–34.
[37] H.K. Forster, N. Zuber, Dynamics of vapor bubbles and boiling heat transfer, AIChE J 1 (1955) 531–535.
[38] K. Nishikawa, Y. Fujita, H. Ohta, S. Hidaka, Effect of the surface roughness on the nucleate boiling heat transfer over the wide range of pressure, in: Int. Heat Transfer Conf. Digital Library, Begel House, 1982.
[39] J.H. Lienhard, A semi-rational nucleate boiling heat flux correlation, Int. J. Heat Mass Transf. 6 (1963) 215–219.
[40] C.L. Tien, A hydrodynamic model for nucleate pool boiling, Int. J Heat Mass Transf. 5 (1962) 533–540.
[41] B.B. Mikic, W.M. Rohsenow, A new correlation of pool-boiling data including the effect of heating surface characteristics, J. Heat Transf. 91 (1969) 245–250.
[42] D.A. Labuntsov, Heat transfer problems with nucleate boiling of liquids, Ther. Eng. (USSR) English translation 19 (1972) 21–28.
[43] K. Stephan, M. Abdelsalam, Heat-transfer correlations for natural convection boiling, Int. J. Heat Mass Transf. 23 (1980) 73–87.
[44] M. Shiraishi, K. Kikuchi, T. Yamanishi, Investigation of heat transfer characteristics of a two-phase closed thermosyphon, J. Heat Recovery Syst. 1 (1981) 287–297.
[45] H. Imura, H. Kusuda, J.I. Ogata, T. Miyazaki, N. Sakamoto, Heat transfer in two-phase closed-type thermosyphons, JSME Trans 45 (1979) 712–722.
[46] M.G. Cooper, Saturated nucleate pool boiling-a simple correlation, in: 1st UK National Heat Transfer Conf., 1984, pp. 785–793.
[47] D. Gorenflo, P. Sokol, S. Caplanis, Pool boiling heat transfer from single plain tubes to various hydrocarbons, Int. J. Refrig. 13 (1990) 286–292.
[48] W. Leiner, Heat transfer by nucleate pool boiling—General correlation based on thermodynamic similarity, Int. J. Heat Mass Transf. 37 (1994) 763–769.
[49] D. Gorenflo, H_2 Pool boiling, VDI Heat Atlas, Springer, 1994.
[50] I. Pioro, Boiling heat transfer characteristics of thin liquid layers in a horizontally flat two-phase thermosyphon, in: Preprints of 10th Int. Heat Pipe Conf., Stuttgart, Germany, 1997, pp. 1–5.
[51] I.L. Pioro, W. Rohsenow, S.S. Doerffer, Nucleate pool-boiling heat transfer. II: assessment of prediction methods, Int. J. Heat Mass Transf. 47 (2004) 5045–5057.
[52] I.L. Mostinski, Application of the rule of corresponding states for calculation of heat transfer and critical heat flux, Teploenergetika 4 (1963) 66–71.
[53] G.N. Danilova, Correlation of boiling heat transfer data for Freons, Heat Transf. – Sov. Res 2 (1970) 73–78.
[54] K. Bier, J. Schmadl, D. Gorenflo, Influence of heat flux and saturation pressure on pool boiling heat transfer of binary mixtures, VT Verfahrenstechnik 16 (1982) 708–710.
[55] T. Ueda, T. Miyashita, P. Chu, Heat transport characteristics of a closed two-phase thermosyphon, JSME Int. J. 32 (1989) 239–246.
[56] U. Gross, Pool boiling heat transfer inside a two-phase thermosyphon correlation of experimental data, in: Int. Heat Transfer Conf. Digital Library, Begel House, 1990.
[57] F. Kaminaga, Y. Okamoto, T. Suzuki, T. Ma, Study on boiling heat transfer correlation in a closed two-phase thermosyphon, in: Proc. 8th Int. Heat Pipe Conf., Beijing, 1992.
[58] F.M. Chowdhury, F. Kaminaga, K. Goto, K. Matsumura, Boiling heat transfer in a small diameter tube below atmospheric pressure on a natural circulation condition, J. Japan Ass. for Heat Pipe 16 (1997) 14–16.
[59] M.S. El-Genk, H.H. Saber, Heat transfer correlations for small, uniformly heated liquid pools, Int. J. Heat Mass Transf. 41 (1998) 261–274.

[60] T. Kiatsiriroat, A. Nuntaphan, J. Tiansuwan, Thermal performance enhancement of thermosyphon heat pipe with binary working fluids, Exp. Heat Transf. 13 (2000) 137–152.
[61] G. Ribatski, J.M.S. Jabardo, Experimental study of nucleate boiling of halocarbon refrigerants on cylindrical surfaces, Int. J. Heat Mass Transf. 46 (2003) 4439–4451.
[62] V. Ganesan, R. Patel, J. Hartwig, I. Mudawar, Universal critical heat flux (CHF) correlations for cryogenic flow boiling in uniformly heated tubes, Int. J. Heat Mass Transf 166 (2021) 120678.
[63] A. Rohatgi, WebPlotDigitizer 2018, Pacifica, CA, 2017.
[64] P.G. Kosky, An Experimental Study of Nucleate Boiling in Saturated Liquid Oxygen and Nitrogen Between Subatmospheric and the Critical Pressures, University of California, 1963.
[65] D.N. Lyon, P.G. Kosky, B.N. Harman, Nucleate boiling heat transfer coefficients and peak nucleate boiling fluxes for pure liquid nitrogen and oxygen on horizontal platinum surfaces from below 0.5 atmosphere to the critical pressures, Adv. Cryog. Eng. 9 (1964) 77–87.
[66] R.W. Graham, R.C. Hendricks, R.C. Ehlers, An experimental study of the pool heating of liquid hydrogen in the subcritical and supercritical pressure regimes over a range of accelerations, Adv. Cryog. Eng. 10 (1965) 342–352.
[67] D.N. Lyon, M.C. Jones, G.L. Ritter, C.I. Chiladakis, P.G. Kosky, Peak nucleate boiling fluxes for liquid oxygen on a flat horizontal platinum surface at buoyancies corresponding to accelerations between− 0.03 and lgE, AIChE J 11 (1965) 773–780.
[68] D.N. Lyon, Boiling heat transfer and peak nucleate boiling fluxes in saturated liquid helium between the lambda and critical temperatures, Adv. Cryog. Eng. 10 (1965) 371.
[69] R.D. Cummings, J.L. Smith, Boiling Heat Transfer to Liquid Helium, Pergamon, 1966.
[70] P.G. Kosky, Studies in Boiling Heat Transfer to Cryogenic Liquids, University of California, Berkeley, 1966.
[71] J.A. Clark, E.W. Lewis, H. Merte Jr, Boiling of liquid nitrogen in reduced gravity fields with subcooling, NASA Report no. CR-98248 (1967).
[72] A.P. Butler, G.B. James, B.J. Maddock, W.T. Norris, Improved pool boiling heat transfer to helium from treated surfaces and its application to superconducting magnets, Int. J. Heat Mass Transf. 13 (1970) 105–115.
[73] H. Merte, Incipient and Steady Boiling of Liquid Nitrogen and Liquid Hydrogen Under Reduced gravity, Eng. College Tech, Univ. Michigan, 1970. Report.
[74] M. Jergel, R. Stevenson, Static heat transfer to liquid helium in open pools and narrow channels, Int. J. Heat Mass Transf. 14 (1971) 2099–2107.
[75] V.A. Grigoriev, Y.M. Pavlov, E.V. Ametistov, An investigation of nucleate boiling heat transfer of helium, Int, in: Heat Transfer Conf. Digital Library, Begel House, 1974.
[76] M. Jergel, R. Stevenson, Contribution to the static heat transfer to boiling liquid helium, Cryogenics 14 (1974) 431–433.
[77] J.L. Swanson, H.F. Bowman, in: Transient surface temperature behavior in nucleate pool-boiling nitrogen, Int. Heat Transfer Conf. Digital Library, Begel House, 1974.
[78] D. Warner, E.L. Park Jr, Effect of heat transfer surface aging on heat flux in nucleate boiling liquid nitrogen, Adv. Cryog. Eng. 20 (1975).
[79] V.A. Grigoriev, Y.M. Pavlov, E.V. Ametistov, V.I. Antipov, Heat transfer in boiling helium to superconducting elements in power generating equipment, Future energy production systems, Heat and Mass Transfer Processes I (1976).
[80] I.P. Vishnev, V.V. Corokhov, G.G. Svalov, Study of heat transfer in boiling of helium on surfaces with various orientations, Heat Transf. – Soviet Res. 8 (1976) 104–108.
[81] S. Ishigai, M. Kaji, T. Watanabe, A. Yamaji, Boiling heat transfer from horizontal plates to liquid nitrogen under atmospheric pressure, Techno. Rep. - Osaka University 27 (1977) 485–493.
[82] H. Ogata, W. Nakayama, Heat transfer to subcritical and supercritical helium in centrifugal acceleration fields 1. Free convection regime and boiling regime, Cryogenics 17 (1977) 461–470.
[83] E.A. Ibrahim, R.W. Boom, G.E. McIntosh, Heat transfer to subcooled liquid helium, Adv. Cryog. Eng. 23 (1978) 333–339.
[84] B.I. Verkin, Y.A. Kirichenko, S.M. Kozlov, K.V. Rusanov, Heat transfer during pool boiling of subcooled helium, in: Proc. 8th Int. Cryog. Eng. Conf., Genova, Italy, 1980, pp. 256–260.
[85] H. Ogata, W. Nakayama, Heat transfer to boiling helium from machined and chemically treated copper surfaces, Adv. Cryog. Eng. 27 (1982) 309.
[86] S. Nishio, Study on minimum heat-flux point during boiling heat transfer on horizontal plates, Trans. JSME 51 (1985) 582–590.
[87] C. Beduz, R.G. Scurlock, A.J. Sousa, Angular dependence of boiling heat transfer mechanisms in liquid nitrogen, Adv Cryog Eng. 33 (1988) 363–370.
[88] G.R. Chandratilleke, S. Nishio, H. Ohkubo, Pool boiling heat transfer to saturated liquid helium from coated surface, Cryogenics 29 (1989) 588–592.
[89] S. Nishio, G.R. Chandratilleke, Steady-state pool boiling heat transfer to saturated liquid helium at atmospheric pressure, JSME Int. J. 32 (1989) 639–645.
[90] S.P. Ashworth, C. Beduz, J. Mayne, A. Pasek, R.G. Scurlock, Evaluation of a novel enhanced boiling surface in cryogenic liquids, Adv. Cryog. Eng. 35 (1990) 429–435.
[91] Y.A. Kirichenko, S.M. Kozlov, K.V. Rusanov, E.G. Tyurina, Heat transfer crisis during liquid nitrogen cooling of high temperature superconductor, Cryogenics 31 (1991) 979–984.
[92] S.M. Kozlov, S.V. Nozdrin, Heat transfer and boundaries of its regimes during hydrogen boiling at different metallic surfaces, Cryogenics 32 (1992) 245–248.
[93] H. Ogata, H. Mori, Steady state heat transfer in transition boiling of helium on copper surfaces, Cryogenics 33 (1993) 640–642.
[94] A. Iwamoto, R. Maekawa, T. Mito, J. Yamamoto, Steady state heat transfer characteristics in He I with different surface area, Adv. Cryog. Eng. 43 (1998) 1481–1487.
[95] D.N.T. Nguyen, R.H. Chen, L.C. Chow, C. Gu, Effects of heater orientation and confinement on liquid nitrogen pool boiling, J. Thermophys. Heat Trans. 14 (2000) 109–111.
[96] K. Hata, H. Nakagawa, H. Tatsumoto, Y. Shirai, M. Shiotsu, Critical heat flux on a flat plate in a pool of subcooled liquid helium, in: AIP Conf. Proc., Albuquerque, New Mexico, 2002, pp. 1460–1467.
[97] K. Ohira, H. Furumoto, Nucleate pool boiling heat transfer to slush hydrogen, in: Proc. 16th Int. Cryog. Eng. Conf./Int. Cryog. Mat. Conf., Kitakyushu, Japan, 1997, pp. 601–604.
[98] M.C. Duluc, B. Stutz, M. Lallemand, Transient nucleate boiling under stepwise heat generation for highly wetting fluids, Int. J. Heat Mass Transf. 47 (2004) 5541–5553.
[99] T. Jin, J. Hong, H. Zheng, K. Tang, Z. Gan, Measurement of boiling heat transfer coefficient in liquid nitrogen bath by inverse heat conduction method, J. Zhejiang Univ. Sci. 10 (2009) 691–696.
[100] P. Wang, P.L. Lewin, D.J. Swaffield, G. Chen, Electric field effects on boiling heat transfer of liquid nitrogen, Cryogenics 49 (2009) 379–389.
[101] T. Jin, S.Y. Zhang, K. Tang, Y.Z. Huang, Observation and analysis of the detachment frequency of coalesced bubbles in pool boiling liquid nitrogen, Cryogenics 51 (2011) 516–520.
[102] B.V. Balakin, M.I. Delov, K.V. Kutsenko, A.A. Lavrukhin, O.V. Zhdaneev, Heat transfer from Ni–W tapes in liquid nitrogen at different orientations in the field of gravity, Cryogenics 65 (2015) 5–9.
[103] A. Zoubir, R. Agounouna, I. Kadirib, K. Sbaia, M. Rahmounea, Experimental study of the intensification of heat transfer by pool boiling LN2: Application to cooling of a brass ribbon in horizontal position, Front. Heat Mass Transf. 7 (2016) 33.
[104] M. Baldwin, A. Ghavami, S.M. Ghiaasiaan, A. Majumdar, Pool boiling in liquid hydrogen, liquid methane and liquid oxygen: A review of available data and predictive tools, Cryogenics 115 (2021) 103240.
[105] R.F. Barron, G.F. Nellis, Cryogenic Heat Transfer, CRC press, 2016.
[106] R.M. Holdredge, P.W. McFadden, Heat transfer from horizontal cylinders to a saturated Helium-I bath, Adv. Cryog. Eng. 16 (1971) 352–358.
[107] K. Nishikawa, K. Yamagata, On the correlation of nucleate boiling heat transfer, Int. J. Heat Mass Transf. 1 (1960) 219–235.
[108] K. Stephan, P. Preusser, Heat transfer and critical heat flux in pool boiling of binary and ternary liquid mixtures, German Chem. Eng. 2 (1979) 161–169.
[109] R. Raj, J. Kim, J. McQuillen, On the scaling of pool boiling heat flux with gravity and heater size, J. Heat Transf. 134 (2012) 011502.
[110] L. Wang, K. Zhu, F. Xie, Y. Ma, Y. Li, Prediction of pool boiling heat transfer for hydrogen in microgravity, Int. J. Heat Mass Tranf. 94 (2016) 465–473.